between PE and the copolymers, independent of viscosity and thermal energy. A downward shift of the q* versus t^{1/3} is a consequence of decreasing compatibility of the constituent polymer, and hence compatibility of the copolymers with PE follows the sequence EcB > EcO > EaP > PcE.

Discussion

Two principal approaches have been investigated in attempts to describe miscibility in polyolefin blends. In the first approach, mixing has been correlated with the difference in solubility parameter of the constituent polymers,³ i.e. the larger the difference, the lower the compatibility. The focus of the second approach has been to consider differences in polymer main chain stiffness.^{1,5}

Solubility parameters may be calculated from group contribution methods.²⁷ In this work, for the homopolymers solubility parameters, δ , were calculated from the data due to Hoy, tabulated by Cowie, ²⁷ using the following equation: $\delta = \sum F_j/V$, where F_j is the group contribution of functional group j and V is the molar volume of the polymer repeat unit at 443 K. V was obtained as described in the methods section. Data for the copolymers, δ_{Ecc} , were calculated: $\delta_{Ecc} = X_F \delta_{FC} + X_\alpha \delta_{Fc}$, where x is the mole fraction of monomer residue in the copolymer; subscript E denotes ethylene, α represents the α -olefin, and PE and P α refer to the corresponding values of the polyethylene and poly(α -olefin) homopolymers, respectively. The solubility parameters are listed in table 2.3. The differences in the solubility parameters of the components in each blend, $|\Delta\delta|$, where $|\Delta\delta| = |\delta_{FC} - \delta_{Ecc}|$ are given in table 2.2. To correlate $\Delta\delta$ with the coarsening behavior, we arbitrarily selected the q^* value at the mid-point of the q^* versus $t^{1/3}$, which corresponds to the annealing time of 30 minutes. The reciprocal of the product $q^*t^{1/3}$ was

then taken because the $q^*t^{1/3}$ value for the EcB containing samples is infinity, since no coarsening was observed; $1/(q^*t^{1/3})$ is then zero for EcB samples. $1/(q^*t^{1/3})$ is plotted against $|\Delta \delta|$ in Figure 2.10.

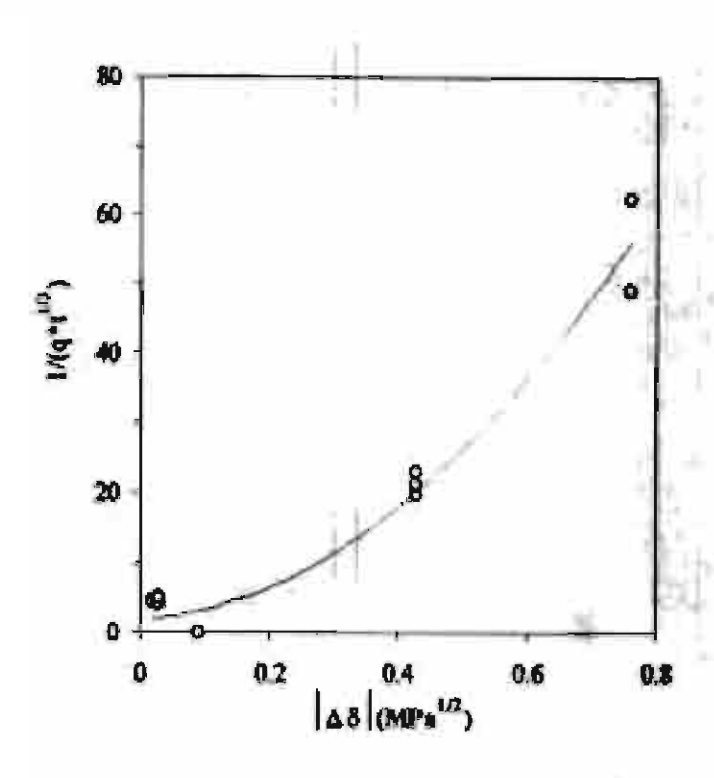


Figure 2:10 Morphology coarsening, represented by $1/(q^{e_1t/3})$, as a function of the difference in solubility parameter of the constituent polymers $|\Delta \delta|$.

Broadly, the larger difference in solubility parameter correlates with more extensive coarsening of the morphologies within the annealing time, as indicated by the higher value of 1/(q*t^{1/3}). However, it fails to reflect the coarser morphologies of the samples containing EcO, in comparison with those containing EcB. Moreover, the increase of branch length in the copolymer, that results from the increase in molecular weight of the α-olefin comonomer residue, brings the solubility parameter of the copolymer closer to that of the PE, suggesting an increase in the compatibility with PE. The morphology analysis shows the opposite result with the EcO copolymer coarsening faster than the EcB containing sample although the former has a lower content of comonomer residue, and

therefore fewer branches. Small angle neutron scattering experiments have shown that χ increases as branch length increases.¹⁹

Chain stiffness may be described using several terms including the characteristic ratio, C. Values of the characteristic ratio were taken from Bicerano²⁸ are listed in Table 2.3. Data for the copolymers were calculated, C_{Eco} , from $C_{Eco} = X_E C_{PE} + X_C C_{PC}$. The differences in the characteristic ratio between the copolymers and the PE, $|\Delta C|$, where $|\Delta C| = |\Delta C_{PE} - \Delta C_{Eco}|$, are shown in Table 2.2; $1/(q^a t^{1/3})$ is plotted as a function of $|\Delta C|$ in Figure 2.11.

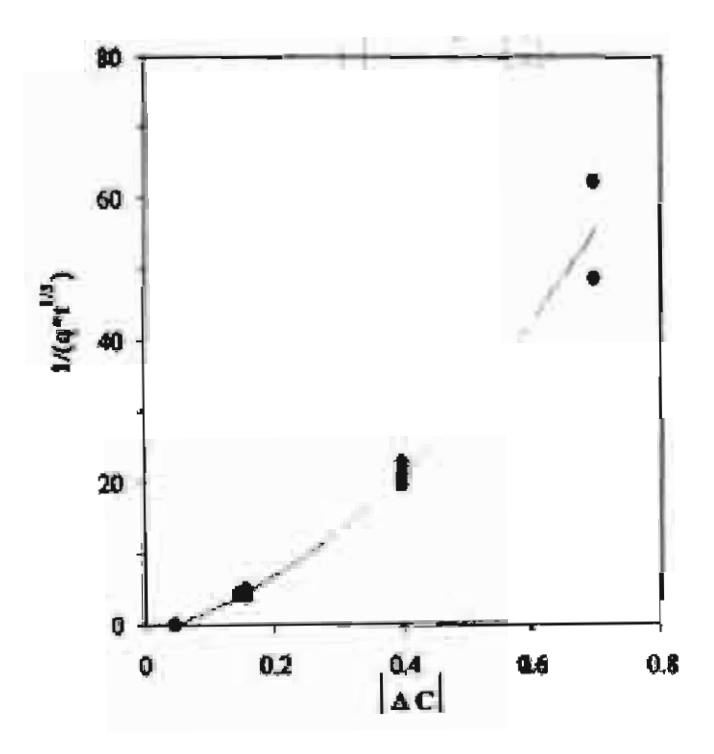


Figure 2.11 Morphology coarsening, represented by $1/(q^*t^{1/2})$, as a function of the difference in characteristic ratio of the constituent polymers $|\Delta C|$.

Apparently, the larger differences in the characteristic ratio are associated with the greater levels of coarsening. Much more data are required to determine the generality of this result, however. Moreover, the correlation between characteristic ratio and solubility

parameter are controlled by the same factors relating to polymer structure and so the results may be confounding of the underlying phenomena that control mixing and coarsening of the polymer blends. As pointed out by Crist and Hill, 19 these simple structural factors, namely solubility parameter and characteristic ratio are inadequate for describing the compatibility of polyolefins when the polymers are very similar in structure and approach the limits of miscibility. As evidenced in this report, the EcO and EcB have close values of solubility parameter and characteristic ratio and yet exhibit markedly different compatibilities with linear PE.

Conclusions

The coarsening rates of linear polyethylene with five poly(ethylene-co-α-olefin) elastomers with compositions at the critical point can be normalized to account for the effects of thermal energy and zero shear rate viscosity. The influence of molecular weight upon the morphology evolution was principally through its effect upon melt viscosity with little effect upon the thermodynamic compatibility. It was revealed that the coarsening progress of the morphology could be related to the copolymer microstructure and branch content. The faster coarsening rates were associated both with the largest differences in solubility parameters and the largest differences in characteristic ratio between polyethylene and the poly(ethylene-co-α-olefin) copolymers. However, the marked differences in coarsening between the EcB and EcO were not well reflected by the small differences in the solubility parameter and characteristic ratio.

Acknowledgements — the authors would like to thank the Thailand research fund for support of this work.

References

- 1. Bates, F. S.; Schulz, M. F.; Rosedale, J. H. Macromolecules 1992, 25, 5547-5550.
- 2. Rhee, J.; Crist B. Macromolecules 1991, 24, 5663-5669.
- 3. Choi, P. Polymer 2000, 41, 8741-8747.
- Krishnamoorti R.; Graessley, W. W.; Balsara N. P.; Lohse, D. J. Macromolecules 1994, 27, 3073-3081.
- 5. Fredrickson, G. H.; Liu, A. J. J Polym Sci Part B: Polym Phys 1995, 33, 1203-1212.
- 6. Yamaguchi, M.; Miyata, H.; Nitta, K. J Appl Polym Sci 1996, 62, 87.
- 7. Thomann, Y.; Suhm, J.; Thomann, R.; Bar, G.; Maier, R. D.; Mulhaupt, R. Macromolecules 1998, 31, 5441.
- 8. Carriere, C. J.; Silvis, H. C. J Appl Polym Sci 1997, 66, 1175.
- 9. Morgan, R. L.; Hill, M.J.; Barham, P. J.; Frye, C. J. Polymer 1997, 38, 1903.
- 10. Hill, M. J.; Barham, P. J. Polymer 1995, 36, 3369.
- 11. Rhee. J.; Crist, B. J Polym Sci Part B: Polym Phys 1994, 32, 159-169.

- 12. Saunders, K. J. Organic chemistry of polymers 2nd edition; Chapman and Hall: London, 1988, pp 46-75.
- 13. Chien, J. C. W.; He, D. J Polym Sci Part A: Polym Chem 1991, 29, 1585-1593.
- 14. Halasa, A. F.; Massie, J. M.; Ceresa, R. J. In Science and technology of rubber 2nd edition; Mark, J. E.; Erman, B.; Eirich, F. R. editors; Academic Press, San Diego, 1994, p 518.
- De Pooter, M.; Smith, P. B.; Dohrer, K. K.; Bennett, K. F.; Meadows, M. D.; Smith,
 G.; Schouwenaars, H. P.; Geerards, R. A. J Appl Polym Sci 1991, 42, 399-408.
- Carreau, P. J., Rheological equations from Molecular Network Theories, Ph.D.
 Thesis, University of Wisconsin, 1968.
- 17. Harris, D. C. J Chem Ed 1998, 75, 119.
- Dumoulin, M. M.; Utracki, L. A.; Carreau, P. J. In Two-phase polymer systems;
 Hanser: Munich, 1991, p 201.
- 19. Crist, B., Hill, M. J. J Polym Sci Part B: Polym Phys 1997, 35, 2329-2353.
- Cowie, J. M. G. Polymers: Chemistry and physics of modern materials 2nd Edition;
 Blackie Academic and Professional: London, 1991, p 265.

- 21 Bicerano, J. Prediction of polymer properties; Marcel Dekker: New York, 1993, pp 66-70.
- 22 Dehoff, R. T. Quantitative microscopy; McGraw-Hill: New York, 1968, p 131.
- 23 Lee, J. K.; Han, C. D. Polymer 1999, 40, 2521-2536.
- 24 Cahn, J. W. J Chem Phys 1965, 42, 93.
- 25 Inaba, N.; Yamada, T.; Suzuki, S.; Hashimoto, T. Macromolecules 1988, 21, 407-414.
- 26 Bartels, C. R.; Crist, B.; Graessley, M. W. Macromolecules 1984, 17, 2702.
- 27 Cowie, J. M. G. Polymers: Chemistry and physics of modern materials 2nd Edition; Blackie Academic and Professional: London, 1991, pp 178-179.
- 28 Bicerano, J. Prediction of polymer properties; Marcel Dekker: New York, 1993, p 286.

The effects of copolymer branching and molecular weight upon the morphology of polypropylene / poly(ethylene-co-α-olefin) blends

Abstract: The coarsening of two-phase morphologies in binary blends comprising two grades of polypropylene and seven poly(ethylene-co-α-olefin) copolymers has been studied. The copolymers had regular structures that differed in molar volume and mole fraction of the α-olefin comonomer residue in the copolymer; monomer residues were derived from propylene, 1-butene, or 1-octene. Molecular weight of the polypropylene and the copolymers was found to affect the coarsening rates of the morphology principally through its influence upon the melt viscosity. The latter effect was largely accounted for through the normalization of the coarsening rate data with respect to the thermal energy and zero shear rate viscosity. Higher molecular weight α-olefin comonomer residues and residue contents in the copolymers led to slower coarsening of the morphology. The copolymers that contained propylene residues exhibited the poorest compatibility with polypropylene. The effect of molecular weight upon the compatibility of the blends was much smaller than the effects of branch length and number of branches.

Introduction

Several publications have considered the influence of poly(ethylene-co-α-olefin) microstructure upon mixing in polyolefin blends. Yamaguchi et al. [1996] used dynamic mechanical analysis to show that in polypropylene / poly(ethylene-co-α-olefin) blends that when the copolymer contained more than 50 mol% of 1-butenc or 1-hexene the

amorphous components of the constituent polymers in the blend were miscible in the solid state. It was inferred from the fine length-scale of samples quenched from the melt that mutual miscibility was also attained in the melt-state. Thomann et al. [1998] concluded that polypropylene formed single phase blends with poly(ethylene-co-1-butene) when the 1-butene content was around 88 wt%, but higher and lower contents resulted in two-phase mixtures. Carriere and Silvis [1997] found that the interfacial tension between polypropylene and poly(ethylene-co-1-octene) copolymers, determined using a fiber retraction method, decreased as the content of 1-octene in the copolymer increased.

About alleran a contract a

1

Two grades of polypropylene (PP) and seven poly(ethylene-co-α-olefin) copolymers were selected for the study. The copolymers used were poly(ethylene-alt-propylene) (EaP), poly(propylene-co-ethylene) (EcP), two types of poly(ethylene-co-1-butene) (EcB), and three grades of poly(ethylene-co-1-octene) (EcO). The EaP, where 'a' denotes alternating, was amorphous, whilst the EcO and EcB had small, broad melting endotherms in DSC analysis centered around 40-50°C. PE was chosen due to the simplicity of its structure and commercial importance. The EcO, PcE, and EcB used were of the metallocene catalyst-type due to their narrow distribution of microstructures. The EaP had a similarly regular structure, being prepared through the catalytic hydrogenation of polyisoprene. The objectives for this section of the work were to separate the effects of polymer molecular weight, melt viscosity, and polymer microstructure upon mixing in polypropylene systems.

Experimental

Materials

The PP samples were prepared using Zeigler-Natta catalysts [Saunders, 1998], whilst the EcO, PcE, and EcB copolymers were synthesized using metallocene single-site catalysts. The EaP copolymer was prepared through the catalyzed addition of molecular hydrogen to polyisoprene. Details of these resins are documented in Table 3.1.

Characterization

Comonomer contents in the copolymers were determined with a Bruker 300 MHz nuclear magnetic resonance spectrometer following the method of Pooter et al. [1991]. Molecular weight data were obtained using a Waters gel permeation chromatograph, employing polystyrene calibration standards in tri-chlorobenzene at 142°C and a refractive index detector. Rheological data were obtained using a Haake RT20 25 mm parallel plate rheometer; nineteen increments in the frequency of the oscillation were made over the range 0.06 to 64.3 rad.s⁻¹. Measurements were made at 443 K under a constant stress of 250 Pa. Zero shear rate complex viscosity, η*₀, was obtained from Carreau's constitutive equation [Carreau, 1968]:

$$\eta_{\omega}^* = \frac{\eta \bullet_0}{(1 + \tau \omega)^n} \tag{1}$$

where η^*_m is the complex viscosity at ω , τ is the reciprocal transition rate, and n is the non-Newtonian exponent; η^*_{0n} τ , and n were found from the unweighted least sum-of-squares method [Harris, 1998] for the fit of the η^*_m values experimentally determined through rheometry upon the model containing ω as the independent variable; i.e.,

Table 3.1 Resin characteristics and their corresponding Carreau equation constants at 443 K

日本の日本の日本日

Reșin	Code	MEI	品	(gcm ⁻³)	α* (mol%)	M., (kgmol ⁻¹)	M _n (kgmol ⁻¹)	η 0 (Pa.s)
Polygropylene	PP1	24"	165	0.905	100	246		852
Polypropylene	PP2	10	165	0.905	100	291		
Polyethylene	Æ	42	130	0.962	0	27	42	1,687
Poly(ethylene-co-1-octene)	Ecol	5.0	53	0.868	7.3	172	22	17.401
Poly(ethylene-co-1-octene)	Ec02	0.5	52	0.868	7.7	261	123	42,183
Poly(ethylene-co-1-octem)	Ec03	1.0	124	0.913	13		·	
Poly(propylene-co-ethylene)	PcE	1	Y	0.860	90	83	,	, = T
Poly(ethylene-co-1-butene)	EcB1	0.8	8	0.880	13	266	120	14,786
Poly(ethylene-co-1-butene)	EcB2	1.2 ^b	8	•	1		V	
Poly(ethylene-alt-propylene)	Eap			0.910	\$	521	314	6.94

ASTM D 1238: 230°C, 2.16 kg

ASTM D 1238: 190°C, 2.16 kg

Density at 25°C

α-olefin content

$$ss_{\min} = \sum_{j=1}^{N} \Delta y_{j}^{2} , \qquad (2)$$

where ss_{min} is the minimum sum of squares of n residuals, Δy , $\Delta y_{\mu} = \eta^{*}_{\mu} - \eta^{*}_{\mu}$, η^{*}_{μ} is the experimental value, and η^{*}_{μ} is the corresponding value calculated from the model for datum j. The Solver program in the Microsoft Excel '97 spreadsheet software was used to accomplish this task. For the EcO2 and EcB1 resins, better fits to the experimental data were obtained using a modified Carreau equation, due to Dumoulin et al. [1991]:

$$\eta_{\bullet} * = \eta_{\bullet} * \left[1 + (\tau \omega)^{\bullet} \right]^{-\alpha}, \tag{3}$$

where m is a fitting constant. The blends, listed in table 2, of PE with the copolymers were prepared with compositions at the critical point, ϕ_2^c , from the Flory-Huggins lattice model, as described by Crist and Hill [1997]:

$$\phi_2^c = \left(1 + (V_2 n_{w2}/V_1 n_{w1})^{\gamma_2}\right)^{-1}, \tag{4}$$

where ϕ_1^c is the volume fraction of copolymer, V_j is the monomer volume, and n_{wj} is the weight average degree of polymerization of component j. Based upon the free volume theory, V_j is a function of the expansion coefficient, β , absolute temperature, T_a and the glass transition temperature, T_a [Bicerano, 1991]:

$$V_{f} = V_{298K} [1 + \beta_{298K} (T - 298)], \tag{5}$$

thermal expansion B298K is the coefficient from: $\beta_{298\pi} = (298 + 4.23T_p^0)^{-1}$. T_g values were determined from the heat capacity versus temperature thermograms obtained using a Perkin Elmer DSC7 differential scanning calorimeter at heating rates of 2, 5, 10, 15, and 30 Kmin'. Tg⁰ values were obtained by plotting T_g versus heating rate and extrapolating to 0 Kmin⁻¹; the T_g axis intercept was taken as the T₂⁰ value. V_{298K} values were taken from Bicerano [1991]. The blends were prepared through dissolution of the components in toluene at 400 K followed by precipitation through pouring into excess methanol at 303 K. The precipitates were removed from the solvent through filtration and then washed with fresh methanol before drying under vacuum at 333 K for 5 hr. The samples were then consolidated, wrapped in aluminum foil, and annealed in an in-house built tube furnace under a nitrogen gas purge for 6 time intervals up to 2 hr at 443 K. A thermocouple was inserted into the sample to determine the temperature. The samples were then quenched in ice-water and were sectioned to a nominal thickness of 1 µm using an RMC microtome operated at -80°C. The sections were placed upon glass slides beneath cover-slips, using di-octylphthalate as the mounting medium, and were viewed using a Nikon E400 light microscope employing phase contrast plates. Images were captured using a Sony CMA-D2CE charge coupled device (CCD) camera. The length-scale of the domains, λ, were measured using Imagepro software using standard stereological analysis [Dehoff, 1968]. Test lines were placed over the image and the length of the test line, xj, traversing each domain was determined. The length scale was then calculated $\lambda = \sum x_j/n_j$, where n_j is the number of times the test line crosses a domain.

Table 3.2 Polymer characteristics

Polymer	α (mol%)	T _g ^{Q_g} (K)	δ ^b (MPa ^{IΩ})	С
PE	0	253.2	14.30	7.00°
PPI	0	278.0	13.43	6.20
PP2	0	278.0	13.43	6.20°
PIB	0	7.11	13.65	6.60
PIO	0	-	13.97	9.10°
EaP	50	201.3	13.87	6.60d
EcO1	7.3	201.2	14.28	7.15 ^d
EcO2	7.7	201.2	14.28	7.16
EcQ3	1.3	•	-	*
EcB1	7		-	-
EcB2	13	241.8	14.22	6.95
PcE	88	248.2	13.54	6.30

Glass transition rate at zero heating rate

Table 3.3 Compositions and zero-shear-rate viscosities at 443 K

Blend	ø :	70 (Pa.s)
PP1/EcB1	0.43	35,436
PP1/EcB2	0.49	12,008
PP1/EcO1	0.53	-
PP1/EcO3	0.49	9,260
PP1/EaP	0.42	5,457
PP2/EcO2	0.57	4,325
PP2/EcP	0.50	37,367
PP2/PcE	0.65	592

Solubility parameter at 170°C calculated from group contributions [Cowie, 1991]

^{*}Characteristic ratio data due to Bicerano [1993]

Calculated from the values of the homopolymers

Results

The $T_{\rm g}^{0}$ values used to calculate the monomer volumes are documented in table 3.2. Since χ has been found a function of blend composition, particularly at low and high concentrations of polymer 2 where a 2-fold increase may occur, the samples in this work were prepared at the critical composition to limit this effect, as documented in table 3.3.

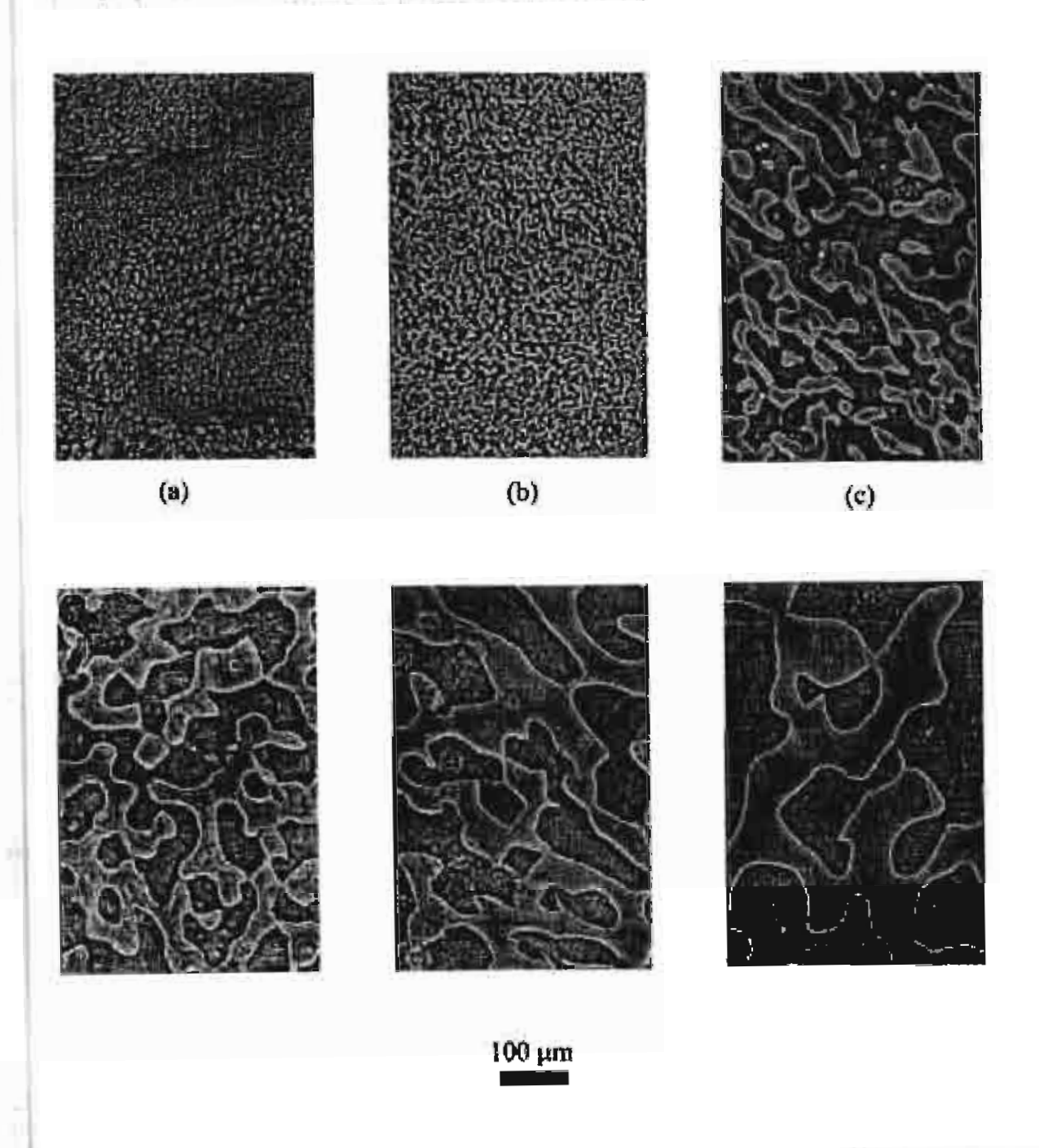


Figure 3.1 CCD camera images, taken with a phase-contrast plate, of PP1/EcO3 after annealing times of (a) 5, (b) 15, (c) 30, (d) 60, (e) 90, and (f) 120 min at 443 K.

Upon annealing under quiescent conditions in the melt state at 443 K, the morphologies that formed were co-continuous. Figure 3.1 shows digitized images of the PP1/EcO3 blend after annealing at 443 K for time intervals of up to 2 hours. Coarsening curves for PP matrices are shown in Figures 3.2 to 3.4.

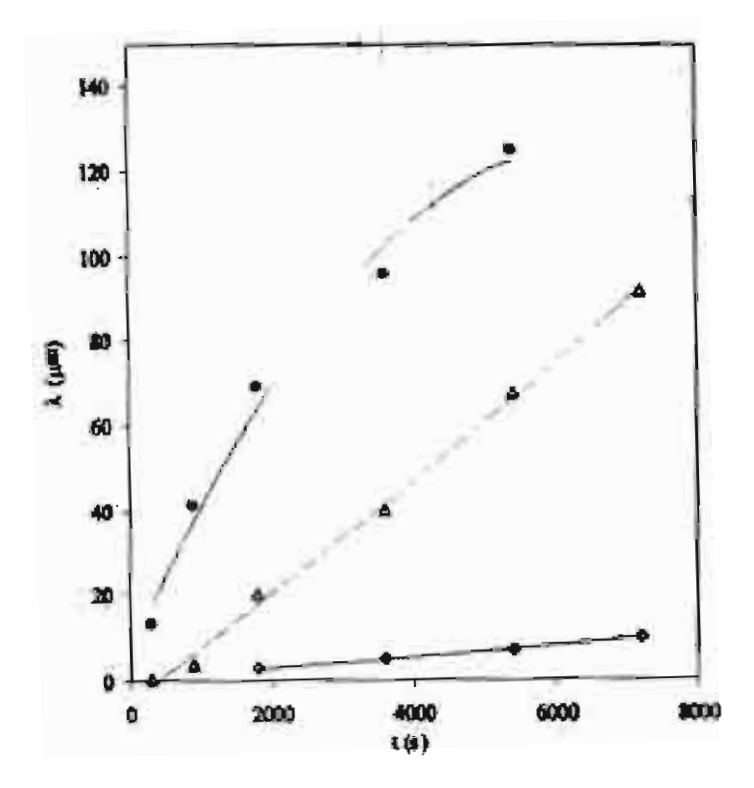


Figure 3.2 Coarsening curves for PP samples blended with (•) PE14, (Δ) PeaP, and (0) PeE.

As discussed in previous sections, the length scale of the morphology, λ , was related to vector, q, by $\lambda = 2\pi/q$.

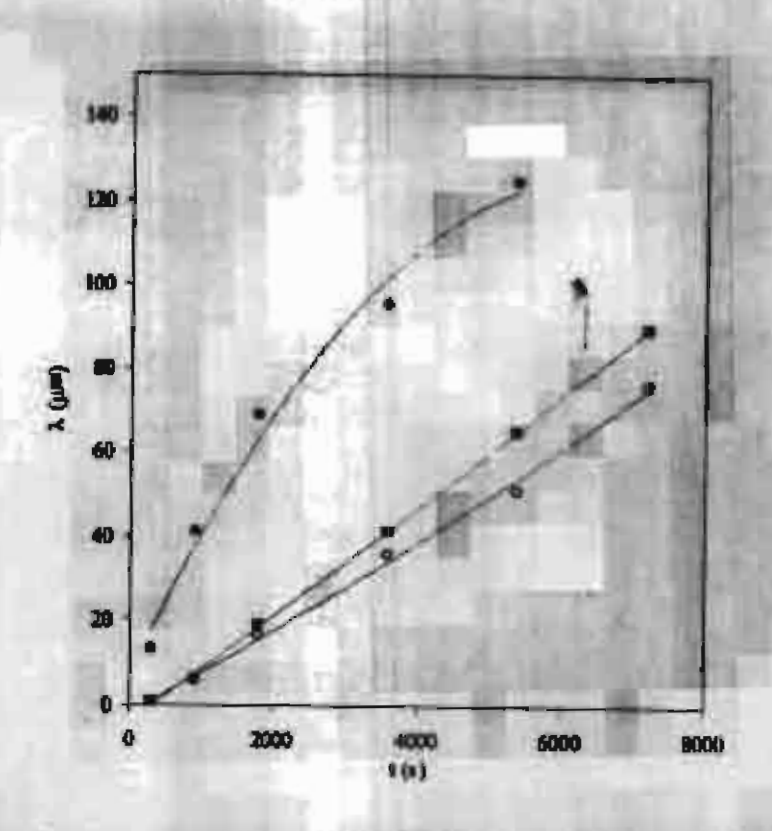


Figure 3.3 Coarsening curves for PP samples blended with (•) PE14, (•) EcB2, and (o) EcB1.

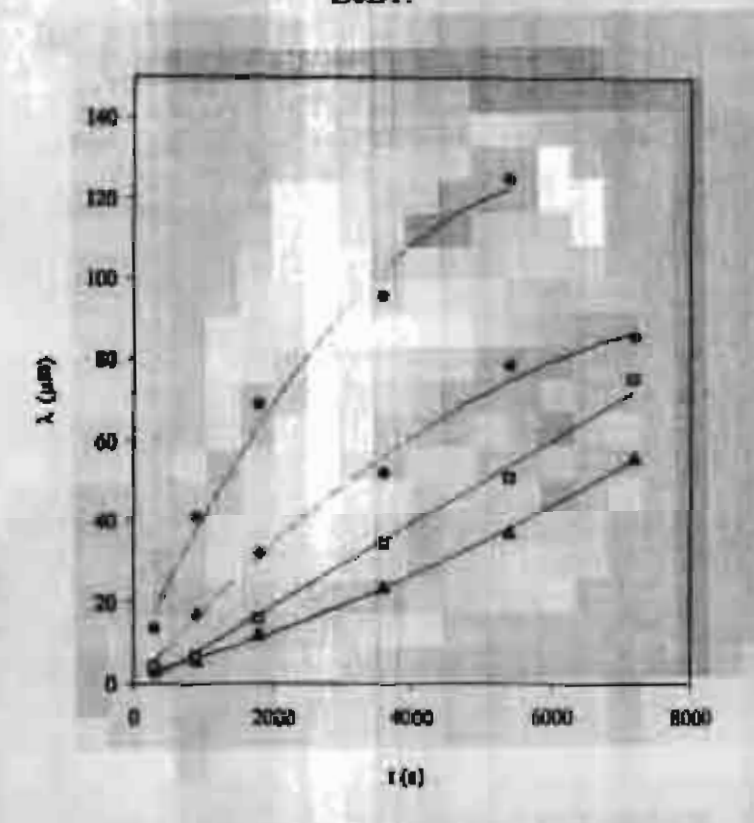


Figure 3.4 Coarsening curves for PP samples blended with (•) PE14, (◆) EcO3, (E1)

EcO2, and (▲) EcO3.

Hydrodynamic effects during the early stage and late stages of coarsening may be described by $\lambda \propto (k_B T/\eta_0)^{1/2} t^{1/2}$ and $\lambda \propto (\Gamma_{1,2}/\eta_0) t$, respectively, where k_B is the Boltzmann constant. Thus, the coarsening rates are affected by the melt viscosity and the thermal energy, as well as the mutual compatibility of the blend components. A normalized term, q^* , may be defined $q^* = q(k_B T/\eta_0)^{1/2}$ that encompasses thermal energy, $k_B T$, and viscous factors, in the form of η_0 . The product $q^* t^{1/3}$ at any time, t, then is a dimensionless number that represents the coarseness of the morphology, independent of viscosity and thermal energy.

The normalized value, q*, is plotted as a function of the cubed root of time in Figure 3.5, 3.6, and 3.7.

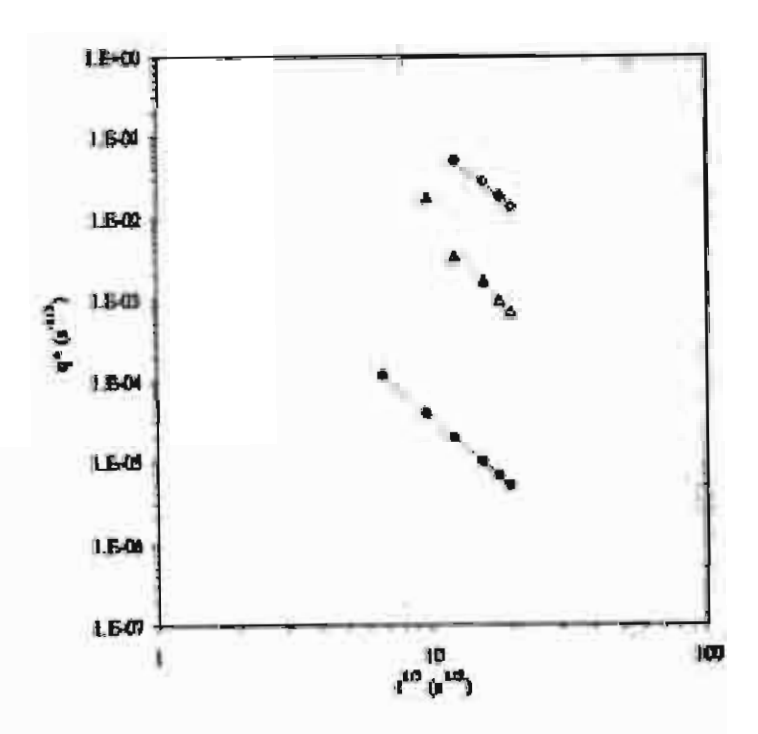


Figure 3.5 Normalised coarsening curves for PP samples blended with (•) PE14, (Δ)

PeaP, and (◊) PcE.

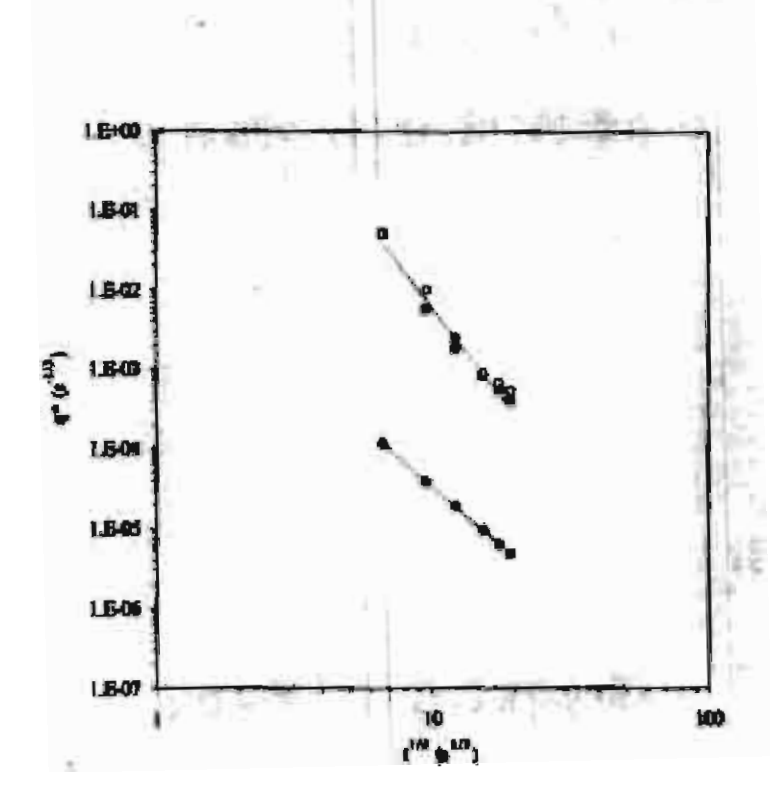


Figure 3.6 Normalised coarsening curves for PP samples blended with (●) PE14, (■)

EcB2, and (o) EcB1.

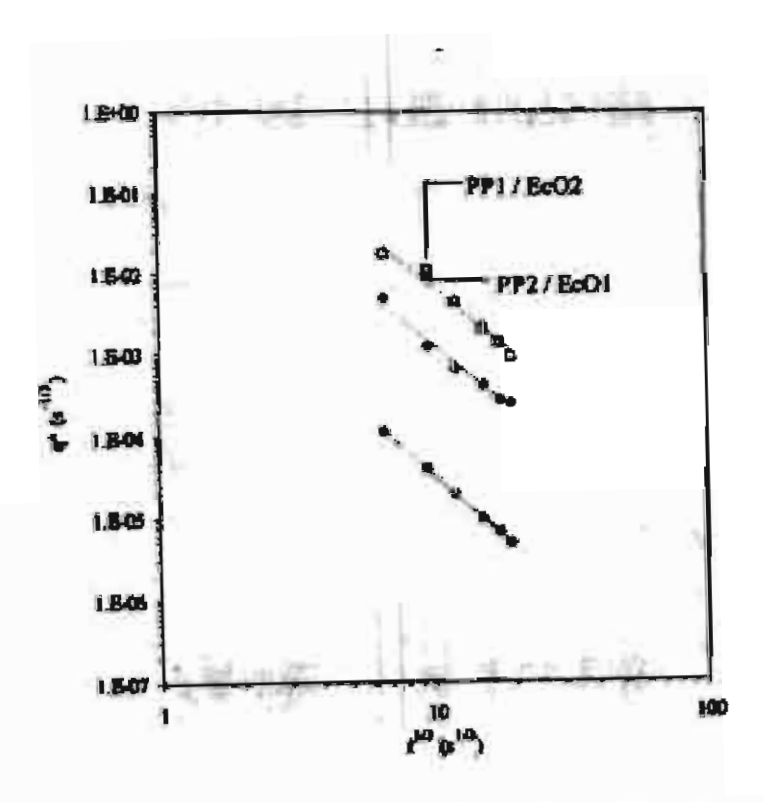


Figure 3.7 Normalised coarsening curves for PP samples blended with (◆) PE14, (◆) EcO3, (□) EcO2, and (▲) EcO3.

As explain in parts one and two, the gradient and relative position of the normalized coarsening curves are determined by the nature of the copolymer. Thus normalization of the data in the form of the term q* largely accounts for the differences in melt viscosity of the PP and copolymer resins, revealing the influence of the copolymer microstructure. Moreover, the result shows that the molecular weights of the resins have a relatively small effect upon the coarsening of the morphology, in comparison with the influence of copolymer microstructure.

Conclusions

The coarsening rates of polpropylene with a range of poly(ethylene-co-α-olefin) elastomers with compositions at the critical point can be normalized to account for the effects of thermal energy and zero shear rate viscosity. As was shown for the polyethylene containing samples, the influence of molecular weight upon the morphology evolution was principally through its effect upon melt viscosity with little effect upon the thermodynamic compatibility. At a given componer concentration, faster coarsening rates were caused by a decrease in the molecular weight of the component.

References

Bicerano, J. Prediction of polymer properties; Marcel Dekker: New York, [1993], p 286.

Bicerano, J. Prediction of polymer properties; Marcel Dekker: New York, [1993], pp 66-70.

Carreau, P. J., Rheological equations from Molecular Network Theories, Ph.D. Thesis,
University of Wisconsin, [1968].

Carriere, C. J.; Silvis, H. C. J Appl Polym Sci [1997], 66, 1175.

Cowie, J. M. G. Polymers: Chemistry and physics of modern materials 2nd Edition;

Blackie Academic and Professional: London, [1991], pp 178-179.

Crist, B.; Hill, M. J. J Polym Sci Part B: Polym Phys [1997], 35, 2329-2353.

Dehoff, R. T. Quantitative microscopy; McGraw-Hill: New York, [1968], p 131.

Dumoulin, M. M.; Utracki, L. A.; Carreau, P. J. In Two-phase polymer systems; Hanser: Munich, [1991], p 201.

Harris, D. C. J Chem Ed [1998], 75, 119.

De Pooter, M.; Smith, P. B.; Dohrer, K. K.; Bennett, K. F.; Meadows, M. D.; Smith, C. G.; Schouwenaars, H. P.; Geerards, R. A. J Appl Polym Sci [1991], 42, 399-408.

Saunders, K. J. Organic chemistry of polymers 2^{ed} edition; Chapman and Hall: London, [1988], pp 46-75.

Thomann, Y.; Suhm, J.; Thomann, R.; Bar, G.; Maier, R. D.; Mulhaupt, R. Macromolecules [1998], 31, 5441.

Yamaguchi, M.; Miyata, H.; Nitta, K. J Appl Polym Sci [1996], 62, 87.

General Discussion

Two principal approaches have been investigated in attempts to describe miscibility, and immiscibility, in polyolefin blends. In the first approach, mixing has been correlated with the difference in solubility parameter of the constituent polymers [Choi, 2000], i.e. the larger the difference, the lower the compatibility. The focus of the second approach has been to consider differences in polymer main chain stiffness [Bates, 1992; Fredrickson, 1992].

Solubility parameters may be calculated from group contribution methods Bicerano, 1993]. In this work, for the homopolymers solubility parameters, δ, were calculated from the data due to Hoy, tabulated by Cowie [1991], using the following equation: $\delta = \sum F_j / V$, where F_j is the group contribution of functional group j and V is the molar volume of the polymer repeat unit at 443 K. V was obtained as described in the methods sections. Data for the copolymers, δ_{Ecc} , were calculated: $\delta_{Ecc} = X_E \delta_{PE} + X_a \delta_{Pc}$, where x is the mole fraction of monomer residue in the copolymer; subscript E denotes ethylene, a represents the a-olefin, and PE and Pa refer to the corresponding values of the polyethylene and poly(a-olefin) homopolymers, respectively. The differences in the solubility parameters of the components in each blend is $|\Delta\delta|$, where $|\Delta\delta| = |\delta_{RE} - \delta_{RD}|$. To correlate Δö with the coarsening behavior, we arbitrarily selected the q* value at the mid-point of the q versus t 112, which corresponds to the annealing time of 30 minutes. The reciprocal of the product q*t110 was then taken because the q*t100 value for the EcB containing samples is infinity, since no coarsening was observed; 1/(q*t10) is then zero for EcB samples. $1/(q^{\bullet}t^{1/3})$ is plotted against $|\Delta\delta|$ in Figure 4.1, for the PE containing formulations and figure 4.2 for those containing PP.

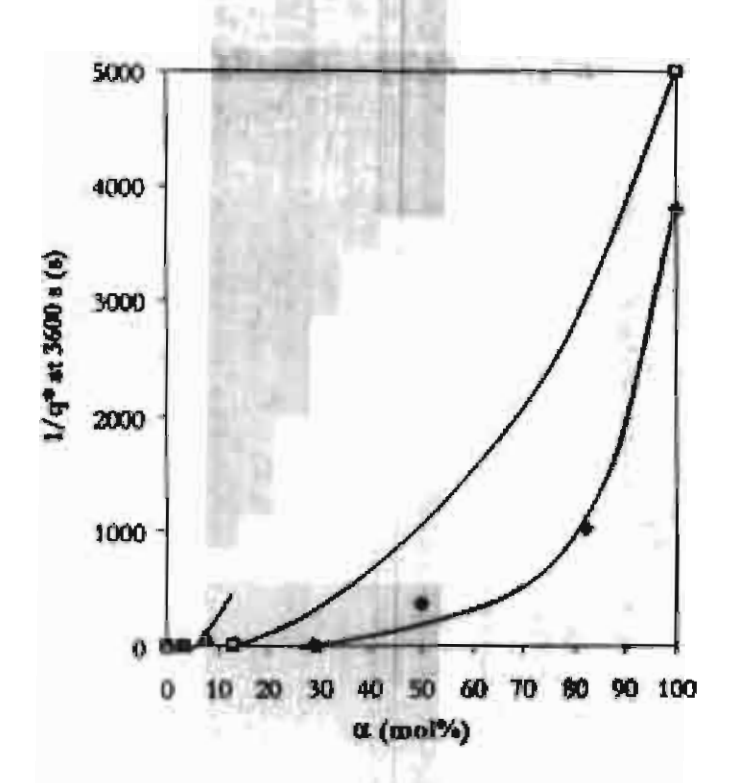
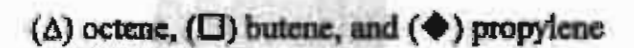


Figure 4.1a Relationship between 1/q* and componer content, a, for PE formulations:



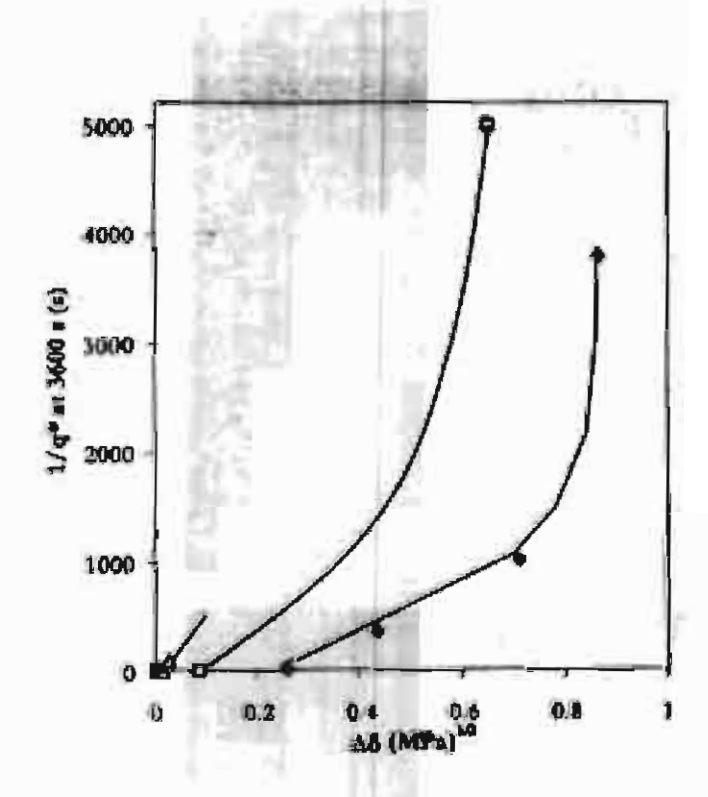


Figure 4.1b Relationship between 1/q* and solubility parameter difference, Δδ, for PE; formulations: (Δ) octene, (□) butene, and (◆) propylene;

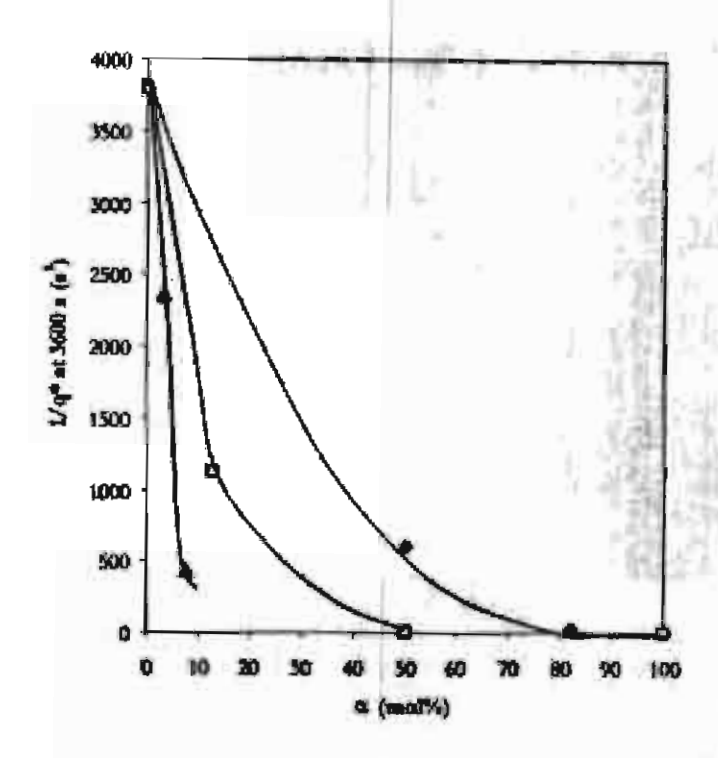


Figure 4.2a Relationship between 1/q* and commonomer content, α, for PP formulations:

(Δ) octene, (□) butene, and (♠) propylene

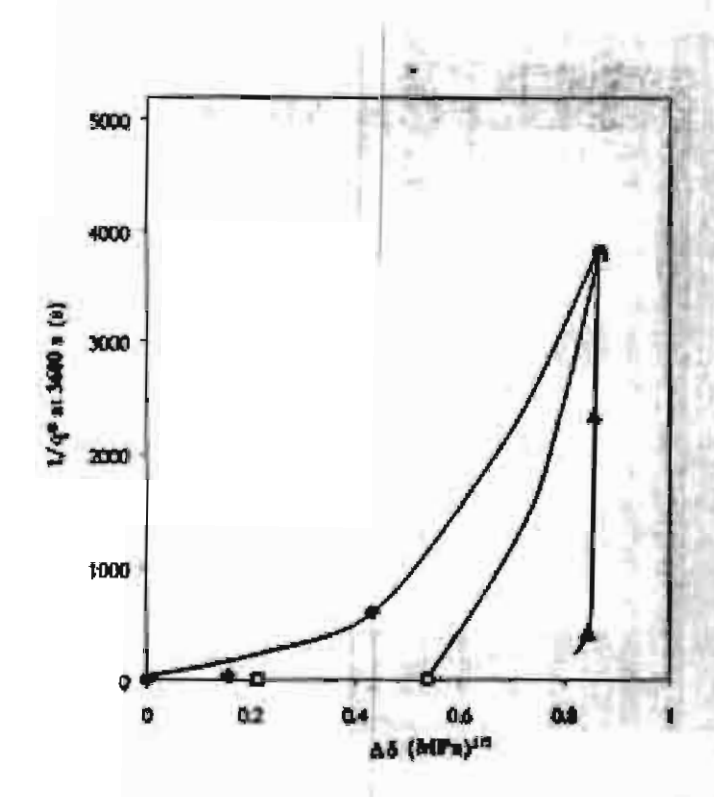


Figure 4.2b Relationship between 1/q* and solubility parameter difference, Δδ, for PP formulations: (Δ) octene, (□) butene, and (♠) propylene

Figure 4.1a comprises the data first shown in figure 2.10 with the extra data point from the PE / PIB blend added. It is evident now that the points are not grouped around a single curve, but may be separated onto different curves depending upon the type of comonomer in the copolymer. From figure 4.1a, it can be seen that for the blends containing PE homopolymers miscibility decreases with increase alpha-olefin content, o. in the copolymer and increasing molecular weight of the alpha-olefin comonomer, as indicated by the higher value of 1/q*. The reverse is apparent in figure 4.2a for the PP homopolymer formulations with miscibility being enhanced when the copolymer has higher concentration of alpha-olefin and higher molecular weight of comonomer, Broadly, when each homopolymer / copolymer series is viewed in isolation, regardless of the type of homopolymer, larger difference in solubility parameter correlates with more extensive coarsening of the morphologies, at a given annealing time. Solubility parameter difference does not reflect differences in morphology coarsening when comparing systems with different alpha-olefin componers, however. There must be structure specific effects present that also affect morphology since there is a clear correlation with comonomer size for systems investigated.

Chain stiffness may be described using several terms including the characteristic ratio; C. Values of the characteristic ratio were taken from Bicerano [1993]. Data for the copolymers were calculated, $C_{Eco.}$ from $C_{Eco.} = X_E C_{Fe.} + X_a C_{Fe.}$. The differences in the characteristic ratio between the copolymers and the PE, $|\Delta C|$, are given by $|\Delta C| = |\Delta C_{Fe.} - \Delta C_{Eco.}|$; L/q^a is plotted as a function of $|\Delta C|$ in Figure 4.3a and 4.3b. As for solubility parameter, the larger differences in the characteristic ratio are associated with the greater levels of coarsening when each homopolymer / copolymer combination is viewed in isolation, except in the case of the PE / EcO system.

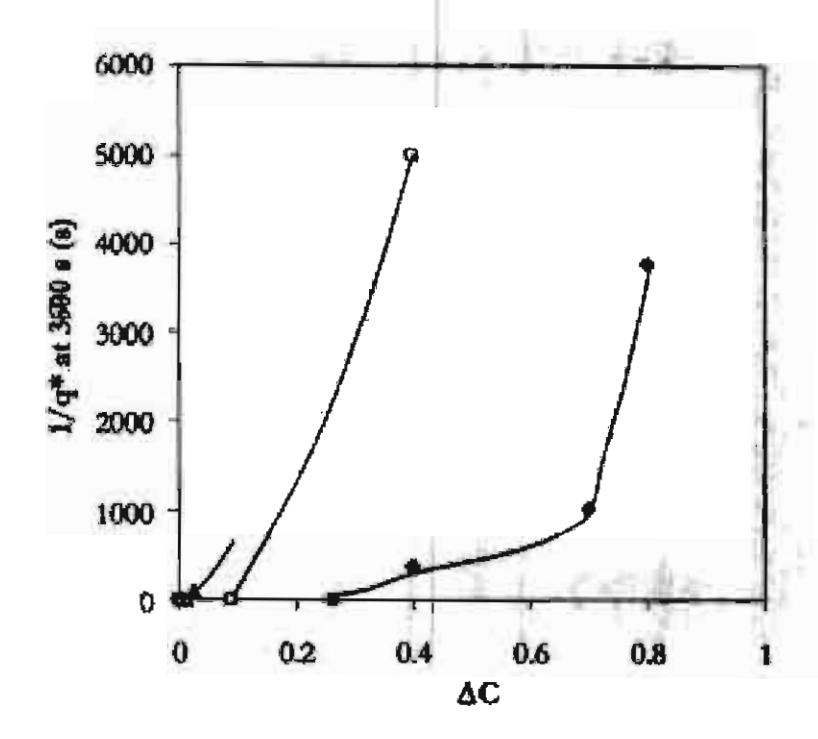


Figure 4.2a Relationship between $1/q^*$ and characteristic ratio difference, $|\Delta C|$, for PE formulations: (Δ) octene, (\Box) butene, and (\spadesuit) propylene

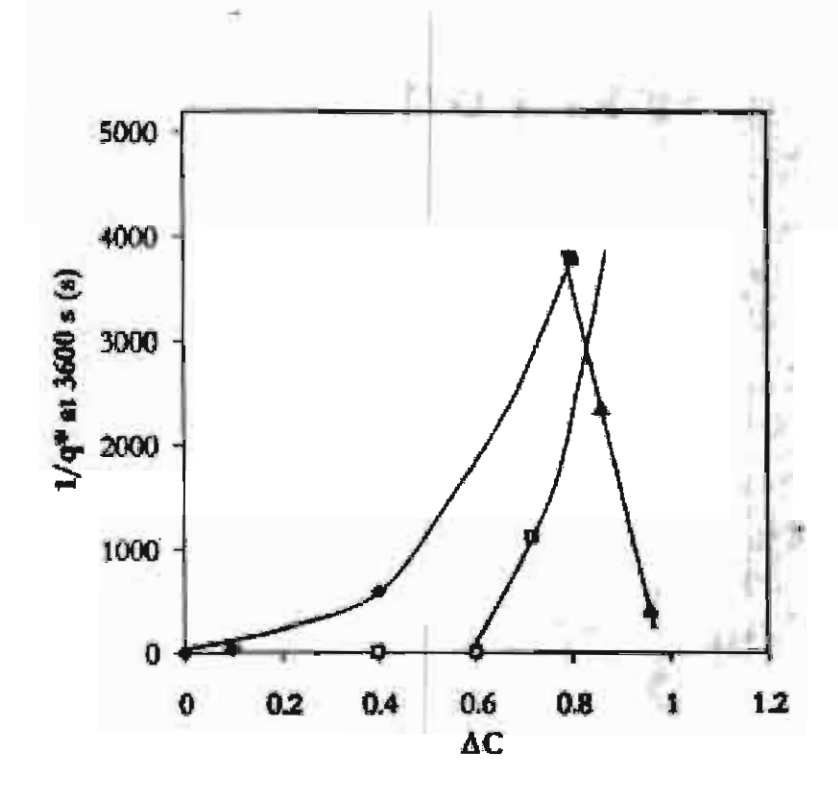


Figure 4.2b Relationship between $1/q^*$ and characteristic ratio difference, $|\Delta C|$, for PP formulations: (Δ) octane, (\Box) butene, and (Φ) propylene

Again, the correlation between 1/q* and characteristic ratio difference suggest specific structural effects. Speculation upon these effects is illustrated in figure 4.3a, in the case of PP homopolymer formulations.

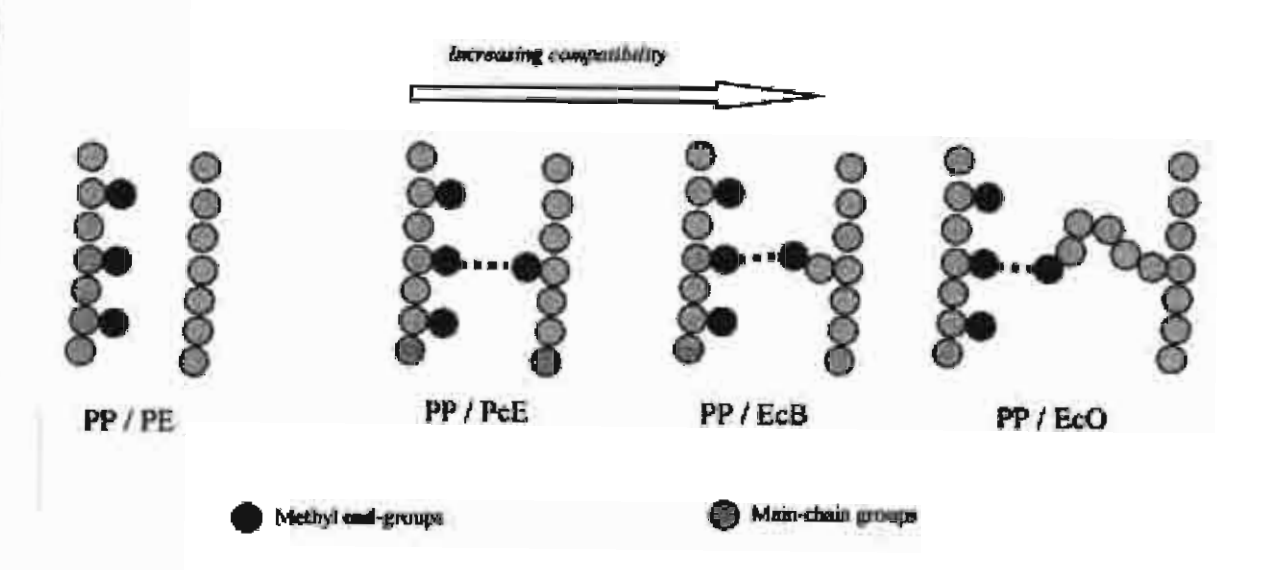


Figure 4.3a Possible associations in the PP homopolymer / copolymer blends

For linear PE, there are very few methyl groups pendent from the main chain and hence PE has weak association with PP leading to the poorest compatibility with PP. In the copolymers, pendent methyl groups are present due to the side-chain of the alpha-olefin. The longer side chains give enhanced compatibility with PP. It is possible that the greater mobility of the longer side chain permits easier association with the PP.

Conversely, for the PE homopolymer formulations, the compatibility with the copolymer decreases as the alpha-olefin branches become longer, as illustrated in figure 4.3b. The PE offers little association with the methyl end-groups of the alpha-olefin. It may be that it is these specific effects that are the major factor in determining miscibility, rather than the overall solubility parameter or chain conformation. Carriere [1997] considered the interfacial tension between PP and poly(ethylene-co-1-octene) copolymers and discussed the results in terms of the number of end groups in the copolymer, an

increase in the number of which led to a decrease in the PP / copolymer interfacial tension. The authors did not consider in detail the effect upon interfacial tension of branch length at constant number of chain ends, however. The results of Carriere et al. are consistent with the results presented herein where it is the activity and nature of the branch ends that most strongly affects the interaction of the homopolymer with each copolymer.

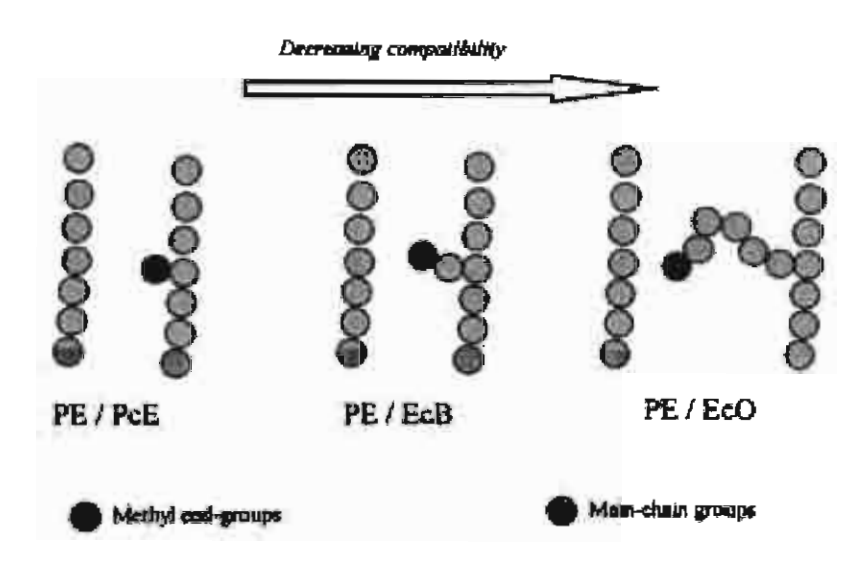


Figure 4.3b Possible associations in the PE homopolymer / copolymer blends

As pointed out by Crist and Hill [1997], these simple structural factors, namely solubility parameter and characteristic ratio are inadequate for describing the compatibility of polyolefins when the polymers are very similar in structure and approach the limits of miscibility. As evidenced in this report, the EcO and EcB have close values of solubility parameter and characteristic ratio and yet exhibit markedly different compatibilities with linear PE.

Conclusions

The compatibility of a series of polypropylene and linear polyethylene homopolymers with a range of poly(ethylene-co-alpha-olefin) copolymers has been investigated through the study of coarsening rates in the melt-state. Kinetic data for samples prepared with compositions at the critical point can be normalized to account for the effects of thermal energy and zero shear rate viscosity. The influence of molecular weight upon the morphology evolution was principally through its effect upon melt viscosity with little effect upon the thermodynamic compatibility. It was revealed that the coarsening progress of the morphology could be related to the copolymer microstructure and branch content. In general, for a given type of copolymer, the faster coarsening rates were associated with both the largest differences in solubility parameters and the largest differences in characteristic ratio between polyethylene and the poly(ethylene-co-aolefin) copolymers. However, the marked differences in coarsening between the EcB and EcO were not well reflected by the small differences in the solubility parameter and characteristic ratio. These results suggest that local interactions are important that are not well described by factors, such as characteristic ratio and solubility parameter, that relate to the overall property of the molecules. Clear correlations were found between the branch length and the number of branches. A higher content of longer branches corresponded to enhanced compatibility with polypropylene homopolymer. Conversely, longer and more numerous branches degraded compatibility in the melt state with linear polyethylene.

References

関門 からのはかる

Bates, F. S.; Schulz, M. F.; Rosedale, J. H. Macromolecules 1992, 25, 5547-5550.

Bicerano, J. Prediction of polymer properties; Marcel Dekker: New York, 1993, pp 66-70.

Carriere, C. J.; Silvis, H. C. J Appl Polym Sci 1997, 66, 1175.

Choi, P. Polymer 2000, 41, 8741-8747.

Cowie, J. M. G. Polymers: Chemistry and physics of modern materials 2nd Edition; Blackie Academic and Professional: London, 1991, pp 178-179.

Crist, B.; Hill, M. J. J Polym Sci Part B: Polym Phys 1997, 35, 2329-2353

Fredrickson, G. H.; Liu, A. J. J Polym Sci Part B: Polym Phys 1995, 33, 1203-1212.

Output

1. International publications

A. Tabtiang, N. Phochalam, and R. Venables, "The effects of copolymer microstructure upon the morphology of polyethylene / poly(ethylene-co-\alpha-olefin) blends'. J. Polym. Sci. B: Polym. Phys. 42(6), (2004), p 965-73.

N. Phochalam, A. Tabtiang, and R. Venables, 'Influence of molecular weight upon the domain coarsening rates in linear polyethylene / poly(ethylene-co-1-octene) blends'. J. Appl. Polym. Sci., 90(6), (2003), p 1655-61

2. Conference papers

Tabliang A, Supatham P, Venables RA. 'The relationship between processing history and the morphology of polyolefins toughened with an elastomeric poly(ethylene-co-1-octene)', in Proc. of the 8th International Seminar on Elastomers, Le Mans, France (2001) p.169.

Phochalam, N., Venables, R.A., Hay, J.N., and Tabtiang A. 'The effects of copolymer microstructure upon the morphology of polyethylene / poly(ethylene-co-a-olefin) blends', Proc. of the PPC-8: 8th Pacific Polymer Conference, Bangkok, Thailand, (2003), p. 130.

Influence of Molecular Weight on the Domain Coarsening Rates in Linear Polyethylene-Poly(ethylene-co-1-octene) Blends

Noree Phochalam, Arunce Tabliang, Richard A. Venables

Faculty of Science, Mahidol University, Rama VI Road, Bangkok 10400, Thailand

Received 29 October 2002, accepted 27 January 2003

ABSTRACT: The coarsening rates of the two-phase morphologies of linear polyethylene/poly(ethylene-or-loctene) blends were determined as functions of molecular weight. Samples with cocontinuous morphologies that were prepared through solution blending were annealed in the melt stare for various times, and subsequently the length scales of the morphologies were determined with a line-intersection method. Length-scale data were multiplied by a function that normalized for the effects of differences in zero-them-one viscosity and thermal energy, after normalization,

the data largely fell on one trend line within the bounds of experimental error. This indicated that the principal effect of increasing molecular weight was to slow the coarsening rate through an increase in melt viscosity, with little effect from the thermodynamic compatibility of the two polymers. D 2003 Wiley Periodicals, Inc. J Appl Polym Sci 90: 1656-1661, 2003

Key words: polyelefins, blends, morphology, metallocene catalysis; polyethylene (PE)

INTRODUCTION

Mixing, phase separation, and domain coarsening affect the morphology and, hence, the properties of polyolefin blends. The principal factors that affect these characteristics in polyolefin blends are molecular weight and the type and level of branching, the latter being largely controlled by the type and quantity of commoner present. The thermodynamics of these systems have been described by an empirical interaction parameter (x) as a function of branch content, where x is found by the fitting of the experimental data to various models. This has been accomplished brough small-angle neutron-scattering studies with random-phase approximation or by cloud-point determination." In the latter approach, because the refractive indices of polyolefins are closely matched, the cloud point could be inferred from the morphology of immeded and quenched samples. The invariance with time of domain size of a fine length scale morphology is indicative of a single-phase melt, whereas increases in domain size on annealing reveal a two-phase melt." Results have been presented, however, where laser light scattering was used to study the length scale (A) of mining and coarsening in blends of isotactic polypropylene and poly(ethylene-co-propylene) and for brends of isotactic polypropylene or syncilotactic polypropylene with poly(ethylene-co-propylene-coethylene norborene).**

One of the explanations of χ was based on regular solution theory, whereby differences in the solubility parameter of the constituent polymers led to an enthalpy-based factor. Several studies on polyolefin blends have shown that the number of branches in the molecule has the most important effect on the determination of the miscibility and compatibility of nonpolar polyolefin blends. It has been proposed that mixing in polyolefin blends may be related to enthalpic considerations that can be described by solubility parameters. Chor calculated the Hildebrand solubility parameters (8's) at elevated temperatures of 1000 simulated carbon models of linear polyethylene (PE) and poly(ethylens-co-I-butens) copolymers, the latter possessing between 10 and 80 ethyl branches per 1000 carbon backbone atoms. An abrupt increase in χ was found in the range 40-50 ethyl branches per 1000 carbon backbone atoms, where y was calculated from $\chi = V_0 R^{-1} T^{-1} (\delta_1 - \delta_2)^2$, where χ is the interaction parameter, V_0 is the reference volume, R is the gas constant, and T is absolute temperature. This was associated with the onset of macroscopic phase separation in the melt state. Krishnamoorti et al. 10 related solubility parameter analysis and solubility parametens determined from pressure-volume-tensperature relationships for a series of blends comprising hydrogenated polydienes, which were used as model polyolefins with different branch types and contents, to their mixing behaviors as determined through smallangle neutron scattering. It was concluded that because solubility parameters could uniquely be as-

Commondator to R. A. Venables (freav@mahidol.ac.th).
Contract grant sponsor: Thailand Research Fund.

Journal of Applied Polymer Science, Vol. 90, 1655–1661 (2009) © 2009 Wiley Periodicals, Inc.

TABLE I sin Characteristics and Their Corresponding

Resin	Sample	(dg min ⁻¹)	(mol %)	(kg aro)-1)	(kg mol ⁻¹)	(Part)	* (a)	nd.
PE	PEI	42	0	101	39	383	0.021	0.465
PE	PE2	14	0	154	•	1,693	2.449	0.186
PE	PE3	0.9	0	234		14,061	1.143	0.312
EcO	EcO1	5.0	7.3	172	78	17,401	_	0.162
EcO	EcO2	0.5	7.3	261	123	42,183	0.001	0.263

M. - weight-average molecular weight, M. - number-average molecular weight.

* MFI = Melt flow index determined in accordance with 85 720A Test condition 4.

ar obefin content.

Reciprocal transition rate of the Carreau equation, eq. (1).

"Slope of the viscosity curve in the pseudoplastic region at \(\gamma \rightarrow \infty \rightarrow \infty. eq. (1).

signed to individual polyolefins, there were no specific pair interactions in most of the blends studied. The two methods of solubility parameter assessment gave numerical agreement with one another. Reductions in the entropy of mixing because of normandom effects that were related to differences in chain conformation and chain stiffness were considered by flates et al.3 The latter effect was described in terms of differences in the statistical segments of the blend constituents that were affected by branch length and commonanter content. Krishnamoorti et al. 10 reported that statistical segment length difference gave an indication of mixing in the melt state, but a clear correlation with the essential parameter in the theory was not established. Evidently, for polyolefin blends close to the limits of miscibility, there is a fine balance of these factors. Continuing from these studies, this study was centered on the influence of chain branching, because of the presence of a comonomer, and molecular weight on the compatibility and morphology of partially miscible polyolefin blands.

The objective of these experiments was to establish the influence of polymer molecular weight on the coarsening rates of the morphologies of selected polyolefin blends. Three commercial grades of high-density polyethylene (PE) and two poly(ethylene-co-1-octene) (EcO) resine that covered a wide range of molecular weights were chosen. PE was chosen because of the simplicity of its structure and its commercial importance.

EXPERIMENTAL

Majerials.

The TE samples were prepared with Zeigler-Natta catalysts." and the EcO samples were synthesized with metallocene single-site catalysts. 2 Details of these resins are documented in Table I.

Characterization

Commonomer contents in the copolymers were determined with a Bruker 300-MHz NMR spectrometer

(Karlsruhe, Germany) following the method of De Pooter et al. 13 Molecular weight data were obtained with a Waters gel permeation chromatograph (Milford, MA), with polystyrene calibration standards in trichlorobenzene at 142°C and a refractive index detector. Differential scanning calorimetry was carried out at heating rates of 5, 10, 15, and 20°C min-1 to determine the glass-transition temperatures $(T_{*}'s)$ of the copolymers with a PerkinElmer DSC-7 (Wellealey, MA). T, at a heating rate of 0°C min was estimated from the temperature axis intercept of the extrapolation to zero heating rate of the plot of T, versus heating rate. Rheological data were obtained with a Hanke KT20 rheometer with oscillating 25-mm parallel plates (Karlsruhe, Germany). Nineteen increments in the angular velocity (a) were made over the range 0.06-64.3 rad s 1. Messurements were made at 170°C under a constant stress of 250 Ps. Zero-shour-rate complex viscosity (va) was obtained from Carreau's constitutive equation:

$$\eta_w^* = \frac{\eta_0^*}{(1+\tau \omega)^n} \tag{1}$$

where η_{α} is the complex viscosity at ω , τ is the relaxation time, and n is the non-Newtonian exponent; no r, and n were found from the unweighted least-sum-of-squares method15 for the fit of the n values experimentally determined through rheometry on the model containing was the independent variable; that is

$$ss_{min} = \sum_{i=1}^{n} \Delta y_i^s \tag{2}$$

where same is the minimum sum of squares of H residuals, Ay, is equal to n' = n n is the experimental value, and no is the corresponding value calculated from the model for datum j. The Solver program in Microsoft Excel '97 spreadsheet software was used to accomplish this task. For the EcO resin, a better fit of the experimental data was obtained with a modified Carreau equation by Dumoulin et al.

TABLE II
Stend Characteristics at 179°C

	100		**	+ (a)	8*	_
Blend	4		(Pas)			7,4
PE1/EcO1	0.43	0.43	910	0.125	0.256	0.022
PE2/EcO1	0.49	0.49	1,486	0.207	0.264	0.097
PE1/EcO2	0.38	0.38	2,570	0.260	D.367	0.009
PEZ/EcO2	0.44	0.43	5,530	0.360	0.463	0.040
PE3/EcOil	0.45	0.48	17,026	1.972	0.268	0.333

*Experimental volume fraction of EcO.

* Reciprocal transition rate of the Carrows equation, eq. 1.

*Slope of the viscosity curve in the pseudoplastic region at 7 → ∞; eq. (1).

"Viscosity ratio, where \u03c3 = \u03c3 (pers) \u03c4 (person)

$$\eta_{\omega}^{s} = \eta_{s} [1 + (r\omega)^{s}]^{-n}$$
 (3)

where m is a fitting constant. The blends, listed in Table II, of PE with the copolymers were prepared with nominal compositions around the critical volume fraction of copolymer, as explained in the Discussion section, nominally around a volume fraction of 0.4.

The blends were prepared through dissolution of the components in tolurne at 127°C followed by precipitation through pouring into excess methanol at 30°C. The precipitates were removed from the solvent through filtration and then washed with fresh methanol and left in the dank of a fume cupboard for I day before they were dried in parase at 80°C for 3 h. The samples were then consolidated and annualed in a in-house constructed tube farmace under a nitrogen gas purge for set times at 170°C. A thermocouple was inserted into the sample to determine the temperature. In some instances, samples were wrapped in aluminum and suspended in a temperature-controlled Hanke recirculating oil bath at 170 ± 0.1°C for various times. The samples were then quenched in ice water and were sectioned to a nominal thickness of 1 pan with an RMC ultramicrotome (Manchester, England) operated at -80°C. The sections were placed upon glass slides beneath cover alips with dioctylphthalate as the mounting medium and were viewed with a Nikon E400 light microscope (Melville, NY) with phase-contrast plates. Images were captured with a Sony CMA-D2CE charged coupled device camera (CCD) and capture board (San Diego, CA). An addiliceral group of blenci samples was amended for 6 h at temperatures in the range 150-358°C in a tube furnace under nitrogen flow. After they were quenched in ice water, flat surfaces were prepared with an RMC ultramicrotome and glass knife at: -80°C. These surfaces were etched with a permanganic acid reagent (1.0% w/v solution at 30°C), following the method of Olley and Basset,17 to selectively remove the amorphous material and were viewed with a Hitachi S-2360N scanning electron microscope (Los Angeles, CA) after vapor deposi-tion with a platimum-palladium alloy.

A of the observed morphologies was determined with imagepro software (Silver Spring, MID). This method is illustrated in Figure 1, with the placement of chords over an image of a PE/EcO blend and the measurement of an intercept length (I), where $\lambda = \sum_{i} I_i/n_i$, shown. Selected microacope images were converted to a frequency-based image by application of the Fourier transform. The frequency-based image comprised a cloud of points, the brightness of which represented the amplitude of the waveform and the position of which represented the frequency of the waveform. If the original image contained a regular pattern, the transformed image would show a regular pattern. For irregular images, a mass of dots would be seen that becomes brighter the closer they were to the center.

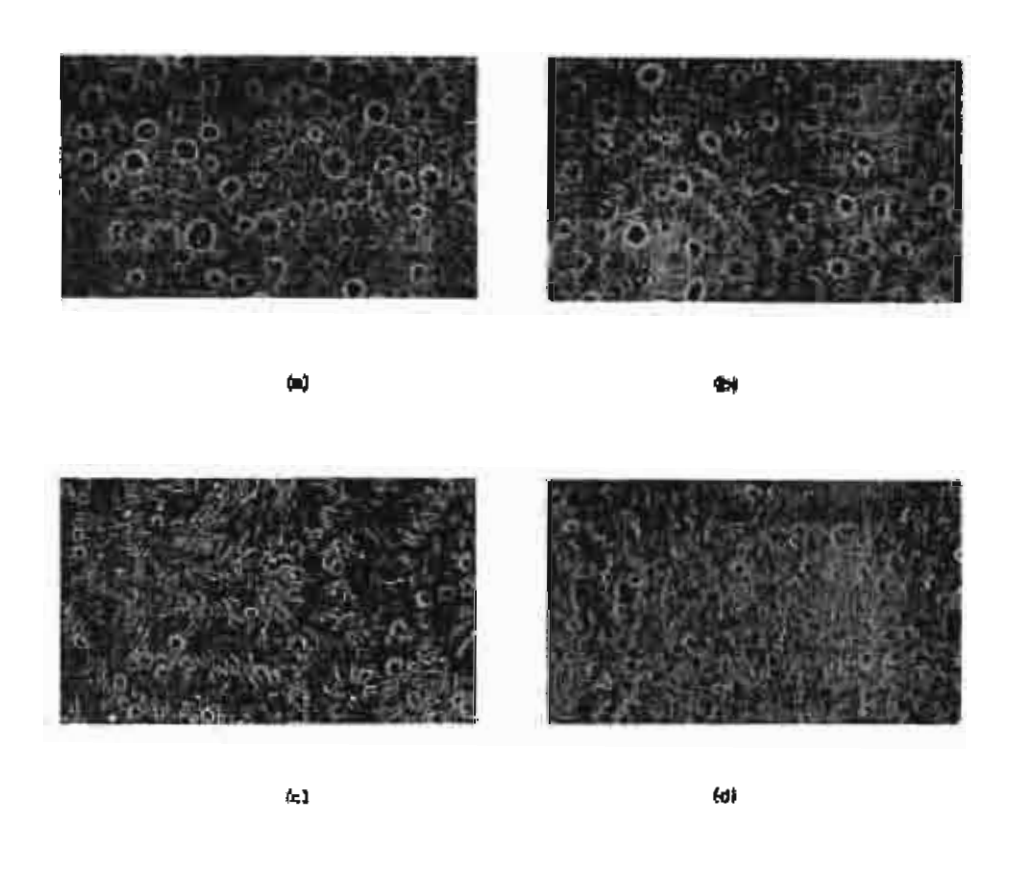
RESULTS AND DISCUSSION

Compatibility of the PE/EcO blend

Blend samples were annealed for various times at temperatures in the range $150-350^{\circ}$ C in a tube furnace to determine the mutual melt-state compatibility of the PE and EcO. These samples were then quenched, microtomed, etched, and viewed with a scanning electron microscope; the resultant micrographs are shown in Figure 2. A plot of the number-average EcO-rich domain diameter (D_n) versus annealing temperature (T_n) , as determined from the micrographs of Figure 2, is displayed in Figure 3. For all of the samples at every temperature, λ of the morphology coarsened on annealing, suggesting that all of the samples were in a two-phase state in the melt because the morphologies coarsened to reduce the interfacial area between the phases and, hence, to minimize the interfacial



Figure 1 Line interception method to find λ of the coordinates morphologies.



3 liw

Figure 2 Scanning electron micrographs of the PEZ/EcO2 blends containing 20 wt % EcO2 after annualing for 6 h at (a) 150, (b) 230, (c) 285, and (d) 320°C

energy, that is, the product of the interfacial tension $(\Gamma_{1,2})$ and the interfacial area. Moreover, the extent of coarsening decreased as T_s increased, even though the mobility of the system increased with increasing tem-

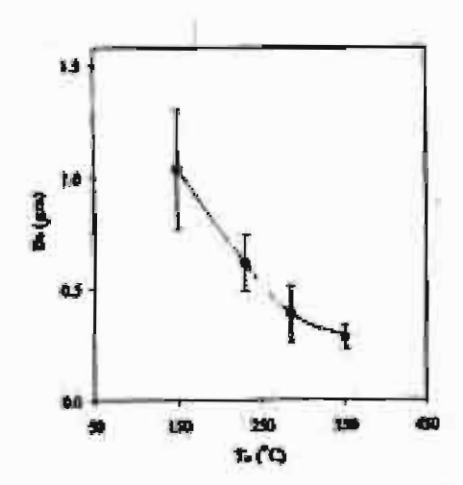


Figure 3 Plot of D_a versus T_a for the PE2/EcO2 blends containing 20 wt % EcO2 after annualing for 6 h at 170°C.

perature because of reduced viscosity, indicating enhanced compatibility at higher temperatures. In an earlier study, 19,20 we concluded that the P62/6cO2 bland was partially miscible because of the observation of PE lamellar crystals in the EcO-rich domains of the morphology. As described by Rhee and Crist,* A of the blend morphology is a function of the ratio χ/χ_c where χ is the polymer-polymer interaction parameter and the subscript c refers to the critical point; that is, the thermodynamic force that drives the morphology to coarsen is weakened as the depth of quench decreases. Thus, for the blends studied herein, a virtual critical point may have been located at a high temperature that was practically inaccessible due the limited thermal stabilities of the constituent polymers. Experiments were limited to 350°C because of the embrittlement of the specimens at temperatures above 350°C. For the T_a range experienced by the samples described herein, that is, in the range 150-320°C, the specimens appeared largely unchanged from their original state, exhibiting slight discoloration and no apparent embrittlement.

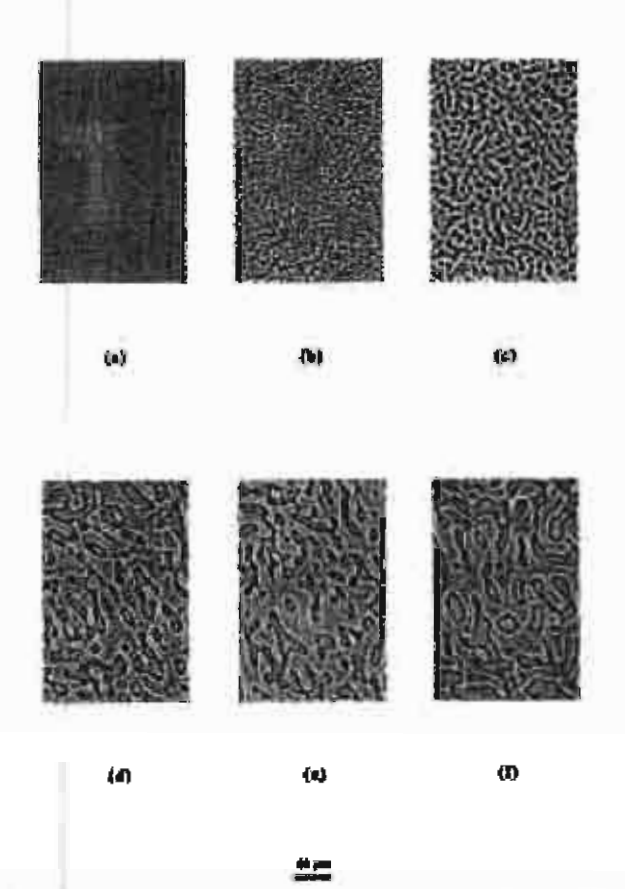


Figure 4 CCD images taken from the transmitted light microscope with a phase-contrast plate. Specimens comprised PEI/EcOI at d. = 0.43 for Ps of (a) 5, (b) 15, (c) 30, (d) 50, (e) 90, and (f) 120 min at 170°C.

Coarsening rates

Because χ has been found to be a function of blend contposition, particularly at low and high concentrations of polymer 2, where π twofold increase may occur, the samples prepared for the coarsening rate study were prepared near the critical composition²¹ to limit this effect; χ is generally near constant at compositions close to the critical point [the critical volume fraction of the EcO copolymer $\{\phi_c\}$] from the Flory-Huggins lattice model:

$$\phi_{\epsilon} = [1 + (V_2 n_{el})^{\epsilon} V_0 n_{el})^{1/2}]^{-1}$$
 (4)

where V_j is the monomer volume and r_{uj} is the weight-average degree of polymerization of component j. On the basis of free-volume theory, V is a function of the expansion coefficient²² (β) and T_{g} :

$$V_{\tau} = V_{\text{conx}}[1 + \beta_{\text{beax}}(T - 298)]$$
 (5)

where β_{290K} is the thermal expansion coefficient at 298 K from

$$\beta_{2md} = (298 + 4.23T_g)^{-1}$$
 (6)

T_g values used were 253 and 203 K for EcO and PE, respectively. On annealing under quiescent conditions in the melt state at 170°C in an oil bath, the morphologies that formed were cocontinuous. Figure 4 shows examples of CCD images of selected PE1/EcO1 blends after annealing for various times. Pigure 5 is an enlargement of a Figure 4(e) that reveals the nature of the phase domains. The phase contrast gave an impression of relief to the image; the apparently recessed regions contained circular ridges because of the presence of PE banded spherulites, identifying these regions as being PE-rich.

 λ 's of the morphologies are plotted as functions of somealing time (!) in Figure 6 for all of the samples prepared with compositions near the critical point. The characteristic λ of the morphology is related to vector q by $\lambda = 2\pi/q$. Plots of q, on a natural logarithmic scale, versus the cubed root of somealing time (!\(^{1/3}\)) were essentially linear in the range 300 < 1 < 7200 s, as shown in Figure 7.

Relationships of this type were discussed by Lee and Han,²⁴ who considered hydrodynamic effects during the early stage and late stages of coarsaning, where

$$\lambda = (k_*T/\pi D^{1/3}p)^{3} \tag{7}$$

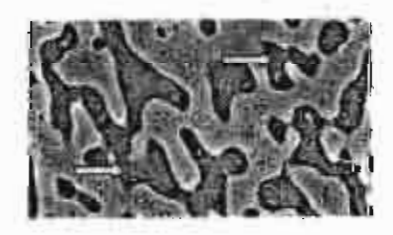
ird

$$\lambda = (\Gamma_{1,2}/\gamma_0^2)t \tag{8}$$

respectively, where $k_{\rm B}$ is the Boltzmann constant and T is the absolute temperature. According to theories of spinodal decomposition²⁵ at times close to t = 0, q has a constant value of $q_{\rm m}$. The data presented here fall in the intermediate stage of coarsening, where λ is function of the cubed root of time. A normalized term $(q^{\rm m})$ may be defined as

$$q^* = q(k_a T/\eta_0^2)^{1/3}$$
 (9)

which accounts for differences in thermal energy (kgT) and viscous factors in the form of no Examples of the



60 mm

Figure 5 CCD image showing the presence of banded spherulites, indicated by arrows, and identifying the PE-rich domains, taken from a transmitted light microscope with a phase-contrast plate. The specimen comprised PE1/EcOl at $\phi_c = 0.43$ armenied for 90 min at 170°C.

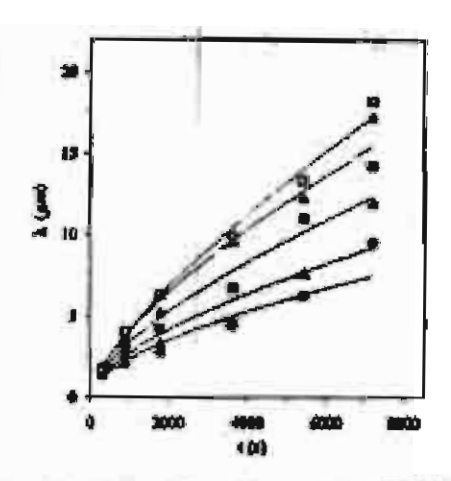


Figure 5 Plot of morphology λ versus t at 120°C for all of the blends prepared at the critical compositions: (W) PE1/ EcO2, (Δ) PE2/EcO2, (Φ) PE3/EcO2, (Ci) PE1/EcO1, and (Δ) PE2/EcO1.

complex viscosity (n°) versus frequency curves for these blends are shown in Figure 8. The q* function is plotted against 1:13 in Figure 9. Apparently, normalization of the data with this function shifted the experimental data to lie close to a single curve, indicating that thermal energy and viscosity effects largely accounted for the differences in coarsening rates. In separate studies, Inaba et al.7 and Lee and Han24 reported that the coarsening in the melt state of immiscible blands after homogenization through dissolution of the constituent polymers in a common solvent and rapid precipitation with a nonsolvent was equivalent to phase separation via spinodal decomposition induced by deep quenching of a melt blend from a single-phase condition into a two-phase conditions through control of temperature and, hence, could be described through established kinetic models. The coarsening rate of the morphology (R) is

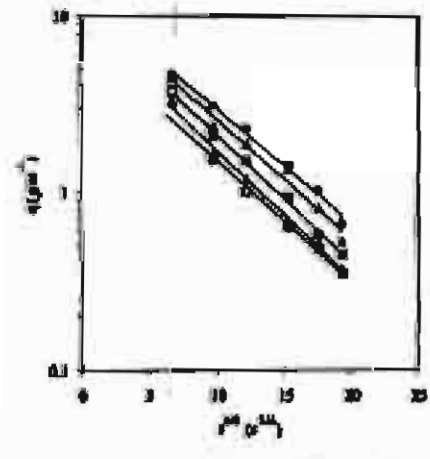


Figure 7 Plot of q versus 1^{1/3} at 170°C for all of the blends prepared at the critical compositions (Ε) PE1/EcO2, (Δ) PE2/EcO2, (Φ) PE3/EcO2, (Δ) PE1/EcO1, and (Δ) PE2/EcO1

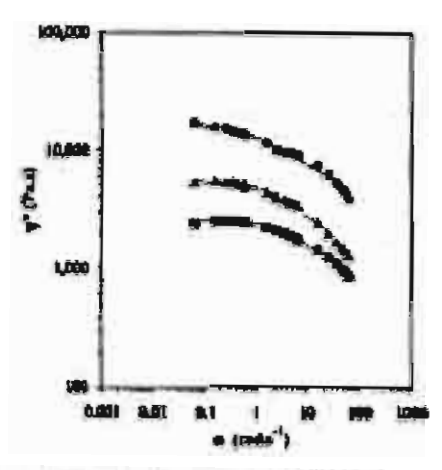


Figure 8 η* versus ω flow curves at 170°C; trend times were calculated with the least-sum-of-squares fit of the Corresu equation to the experimental data: (III) PE1/EcO2, (Δ) PE2/EcO2, and (Φ) PE3/EcO2.

$$R = q^2 D_{\rm ext}/2 \tag{10}$$

where the mutual diffusion coefficient $(D_{\rm app})$ is defined by $D_{\rm app} = D_j f$, in which D_i is the self-diffusion coefficient of polymer j, $D_j = k_j M_{(j)}^{-2}$, M is molecular weight, and

$$f = (x - x_i)/x_i$$
 (11)

and is a factor that modifies the diffusion rates because of thermodynamic effects. ²⁶ In this study, the blend compositions were close to the critical points, and hence, f may have been constant for each system. Zero-shear-rate viscosity and self-diffusion rates are closely related properties, with the term $(D/T)\eta_0$ being insensitive to temperature. Thus, $D_s \partial \eta_0^{-1}$, and, hence, $R \partial D_{app} \partial \eta_0^{-1} f$. Thus, the coarsening rate is largely controlled by the diffusion rate, which is a

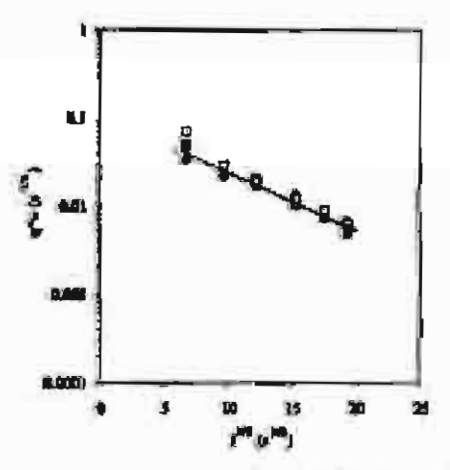


Figure 9 q* as a function of f^{1/2} at 170°C: (***) PE1/EcO2, (***) PE3/ReO2, (***) PE3/ReO2, (***) PE1/EcO1, and (Δ) PE2/EcO1

function of the viscosity with little effect from the influence of molecular weight on the thermodynamic compatibilities of the blend constituents. In the study by Lee and Han24 on the coarsening of the morphologies of immiscible polymer blends, it was explained, on the basis of Cahn's linearized theory of spinodal decomposition, that the length of morphology at very early times of coamening was affected by the molecular weight of the constituent polymers. Higher molecular weights gave larger values of λ in the early stage compared with polymers with low molecular weight. In this work, the blends comprising polymers with the highest molecular weights showed the largest values of q and, hence, the smallest values of λ at the earliest times that were investigated. Moreover, the calculation of q* largely removed the differences in q at the parliest times measured, indicating that at this stage, the coarsening process was controlled by the thermal energy and viscosity, thereby obscuring any effect of molecular weight on λ and q.

Figure 10 shows an image of a PE1/EcO1 blend after 90 min of coarsening. Figure 11 shows the Fourier transform of the image with a ring pattern that indicates the presence of a regular pattern in the CCD image. The dimension of the pattern was of the order of 5 µm, that is, the A of the blend morphology. Evidently, some remnants of the regular morphology produced during rapid precipitation from solution persisted at long i's in the melt state.

CONCLUSIONS

Blends prepared with compositions near the critical point through precipitation from solution formed regular cocontinuous morphologies that annealed at rates determined by the thermal energy and no Data could be normalized with the function q' such that the effects of thermal energy and viscosity largely accounted for differences in coarsening rate and, hence, showed that the differences in molecular weight had

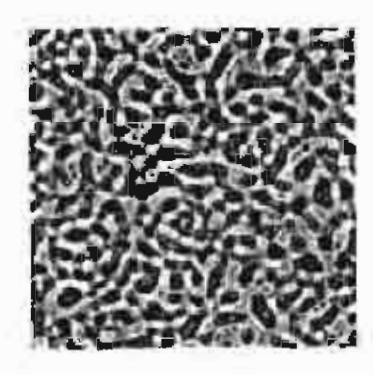


Figure 10 Regular coarsened morphology of a PE1/EcO1 blend prepared at the critical composition.

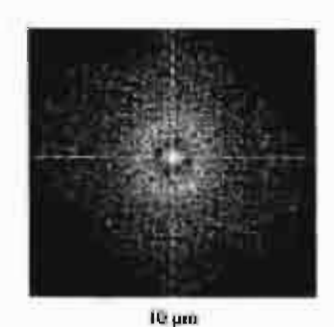


Figure 11 Fourier transform of the image in Figure 10, revealing the regular spacing of the domains in the morphology.

little effect on the compatibility of the blends and, therefore, the morphology.

References

- 1. Mirabella, F. M. J Polym Sci Part B: Polym Phys 1994, 32, 1205
- Rhee, J., Crist, B. J Polym Sci. Part B: Polym Phys 1994, 32, 159.
- 3. Balsara, N. P.; Fetters, L. J.; Flattichmutidis, N.; Lohne, D. J.; Han, C. C.; Gransley, W. W.; Krishnamourti, R. Macromolicules 1992, 25, 6137.
- Weimann, P. A.; Jones, T. D.; Hillmayer, M. A.; Botes, F. S.; Londono, J. D.; Mehrichenko, Y., Wignell, G. D.; Ahndal, K. Macromolecules 1997, 30, 3650.
- Bases, F. S.; Schulz, M. F.; Rosedale, J. H. Muczomobichim 1992, 25. 5547
- Mhee, J.; Crist, B. Macromolecules 1991, 24, 5663.
- 7. Insba, N.; Yamada, T.; Sumiki, S.; Hashimoto, T. Macromolacudes 1988, 21, 407.
- 8. Chin, C. Y.; Yursus, W. M. Z. W.; Chiu, H. W.; Kyo, T. Polymer. 1997, 17, 4433
- Chot, P. Polymer 2000, 41, 8741.
- Krishmanocotti, R.; Genessley, W. W.; Balsara, N. P.; Lohse, D. J. Maryomulecules 1994, 27, 3073.
- 11. Sesseders, K. J. Organic Chemistry of Polymans, 2nd ad.; Chapman & Hall: London, 1988; Chapter 2, p 44
- 12. Chien, J. C. W., He, D. J. J Polym Sci Part A: Polym Chem 1991, 29, 1585.
- 13. De Pooter, M.; Smith, P. II.; Dohner, K. K.; Bennett, K. F.; Mesdows, M. D.; Smith, C. G.; Schouwenners, H. P.; Gerrards, R. A. Appl Polym Sci 1991, 42, 399.
- 14. Carrison, P. J. Ph.D. Thesis, University of Wisconson, 1968.
- 15. Flavors, D. C. J Chem Bd Chem Wiscomain Education 1998, 75, 119.
- 16. Dumoulin, M. bl., Utracki, L. A.; Carrenu, P. J. In Two-Phase Polymer Systems; Utracki, I. A. Ed.; Harres Munich, Germany; Chapter 7, p 201
- 17. Olley, R. H.; Bernet, D. C. Polym Commun 1982, 23, 1707.
- Hill, M. J.; Barbarn, P. J. Polymer 1995, 36, 3369.
- 19. Tabting, A.; Parchana, H.; Versables, R. A.; Inoue, T. J. Polym Sci. Part B: Polym Phys 2001, 39, 380.
- 20. Tabtiang, A.: Parriana, B.: Verrahles, R. A. Polym Plant Technol ling 2001, 40, 423
- 21. Crist, B.; Hill, M. J. J Polyon Sci Part B: Polyon Phys 1997, 35, 2329.
- 22. Cowie, J. M. G. Polymers: Claratistry and Physics of Modern Materials, 2nd ed., Blackle Academic and Professional London. 1991; Chapter 8, p 178.
- 23. Bicerton, J. Prediction of Polymer Properties; Marcel Deldor: New York, 1993; Chapter 3, p 66.
- 24. Lee, J. K.; Hun, C. D. Polymer 1999, 40, 2521.
- Cahn, J. W. J Chem Phys. 1965, 42, 93.
 Okamete, M. Shiomi, K. Inoue, T. Polymer 1995, 36, 87.

Effects of the Copolymer Microstructure on the Morphology of Polyethylene-Poly(ethylene-co-α-olefin) Blends

ARUNIE TABTIANG, NORSE PHOCHALAM, NICHARD VENABLES

Department of Chemistry, Faculty of Science, Mahidol University, Rama VI Road, Bangkok 10400, Thailand

Remitted 21 January 2003; accepted 24 July 2003

ASSERACT: The effects of the copolymor microstructure on the morphology evolution in polysthylene/poly(athylene-co-a-olefin) blends were investigated. Microscopy revealed that the melt-phase morphology, inferred from the solid-state morphologies of annealed and quenched samples, was strongly affected by the copolymer structure, that is, the branch content and branch length. Higher molecular weight a-olefin commoner residues and residue contents in the copolymers led to faster correcting of the morphology. The molecular weight of the polyethylene and the copolymers affected the correcting rates of the morphology, principally through its influence on the melt viscosity. The effects of the molecular weight were largely explained by the normalization of the coursening rate data with respect to the thermal energy and zero-shear-rate viscosity. Thus, the effect of the molecular weight on the competibility of the bloods was much smaller than the effects of the branch length and branch number. O 2004 Wiley Periodicals, Inc. J Polym Sci Part B: Polym Phys 42: 965-973, 2004

Keywoords: polyelefin; blends; copolymer; morphology

INTRODUCTION

Polyoletins comprise long hydrocarbon backbones from which chain branches of various numbers and lengths originate. The length and number of branches affect the ability of a polymer to crystallise and, thorefore, its solid-state properties. Short-chain branching in copolymers based on ethylene, prepared with metallocene catalysts, is principally determined by the type and quantity of a olefus comonomer residues. Properties of polyplefins may be further modified by the blending of resine with different microstructures. Applications range from toughened plastics for whings and films to thermoplastic elastomers. The properties of these blends are affected by the extent of mixing and demixing during processing and are related to the solid-state morphology.

Several studies have investigated the relationship between the polyclefin microstructure and molecular weight and the miscibility of polyplefin blends. 1,3 The two focuses of these studies have been the effects of the solubility parameter $(\delta)^{3,4}$ and the differences in main-chain stiffness and conformation.14 The latter has been described in terms of a statistical segment length that reflects the chain conformation in the melt or under & conditions in solution. These reports suggest that larger differences in 8 and the chain stiffness are associated with reduced mutual miscibility of the constituent polymers in a blend. Both 5 and the main-chain stiffness are directly related to the polymer microstructures, which are a result of the extent of chain branching and the length of chain branches.

Several publications have considered the influence of the poly(ethylene-co-o-olelin) microstructure on mixing in polyolelin blands. Yamaguchi et al. used dynamic mechanical analysis to show that in polypropylene/polytothylene-co-o-olelin)

Correspondence R. Venshies (E-mail: freswinnshidel.sc.th) James of Petrose Sermer Part D. Polymer Physics, Vol. 81, 288-171. (2004) 4 200. Wiley Particular list

blends, when the copolymer contained more than 50 mol % 1-butene or 1-hexene, the amorphous components of the constituent polymers in the blend were miscible in the solid state. It was inferred from the fine length scale of samples quenched from the melt that mutual miscibility was also attained in the melt state. Thomann of al." concluded that polypropylane formed singlephase blends with poly(ethylene-co-1-butene) (EcB) when the 1-butene content was around 88 wt %, but higher and lower contents resulted in two-phase mixtures. Carriers and Silvis found that the interfacial tension between polypropylane and poly(ethylone-co-1-octene) (EcO) copolymers, determined with a fiber retraction method, decreased as the content of 1-octene in the copolymer increased. In the study by Rhee and Crist2 of polyethylene (PE)/hydrogenated polybutadiene blands, in which the latter polymer was used as a model analogue of EcB, it was found that the coarseness of the solid-state morphologies of samples crystallized after melting at temperatures between 150 and 200 °C were a result of the depth of quench from the melt. The depth of quench was described by an interaction perumeter that was proportional to the square of the branch content in the copolymer. Morgan et al." inferred from micrographs of melt-annealed PR/poly(ethylene-co-α-plefin) blends that low levels, around 5 mol %, of 1-butens or 1-octane in the copolymer led to phase separation in the melt state at temperatures between 130 and 170 °C. Above and below these temperatures, singlephase melts were inferred. Hill and Barham 10 followed the kinetics of phase coarsening in blends of different EcO grades containing 2 and 10 mol % 1-octene with microscopy to observe sections of samples that were cooled rapidly from the melt. The morphologies comprised spherical droplet dispersions that coarsened as a function of the cubed root of time.

The morphology of multicomponent PE-based polymer blands affects the toughness properties. With the morphology being a result of the mixing and coarsening processes that take place during melt blanding. In addition to the processing variables that control the thermomechanical bistory of the melt, the morphology is a function of the inherent compatibility of the constituent polymers, the latter being controlled by the differences in the polymer microstructure. Thus, this work was concerned with the influence of the polymer microstructure and molecular weight on the morphology evolution in polyolefin blands in

the two-phase state. Specifically, the objective was to separate the influences of the molecular weight and branch content to assess the relative importance of these factors in the morphology evolution in the melt state. Three grades of highdensity PE and five poly(ethylene-co-z-olefin) copolymers were selected for the study. The copolymers were poly(sthylene-alt-propylene) (EaP). poly(propylene-co-ethylene) (PcE), EcB, and two grades of EcO. EaP, where 'a' denotes alternating, was amorphous, whereas EcO and EcB had small, broad malting endotherms in a differential scanning calorimetry analysis centered around 40-50 *C. PE was chosen for the simplicity of its structure and commercial importance. EcO, PcE, and EcB were metallocene catalysts because of their narrow distribution of microstructures. EaP had a similarly regular structure, being prepared through the catalytic hydrogenation of polyicoprene.

EXPERIMENTAL

Materials

The PE samples were prepared with Zieglar-Natta catalysts, ¹² whereas the EcO, PcE, and EcB copolymers were synthesized with metallocens single-site catalysts. ¹³ The EaP copolymer was prepared through the catalyzed addition of molecular hydrogen to polyisoprene. ¹⁴ The datalis of these resins are documented in Table 1.

Characterization

The component contents in the copolymers were determined with a Bruker 300 MHz nuclear magnetic resonance spectrometer according to the method of De Pooter et al. ¹⁵ Molecular weight data were obtained with a Waters gel permeation chromatograph with polystyrene calibration standards in trichlerobenzene at 142 °C and a refractive-index detector. Rheological data were obtained with a Haake RT20 25-mm parallel-plate rheometer; 19 increments in the frequency of the oscillation were made over the range of 0.05-64.3 rad s⁻¹. The measurements were made at 443 K under a constant stress of 250 Ps. The zero-shear-rate complex viscosity (η^a_{cl}) was obtained from Carreau's constitutive equation:

$$\eta_{\omega}^{\bullet} = \frac{\eta^{\bullet}_{0}}{(1 + \tau \omega)^{\bullet}} \tag{1}$$

Table 1. Ream Characteristics and Their Corresponding Carreen Equation Communication at 443 K.

Resin	Code	MPI*	(g cm **)	(mai %)*	M (kg mol -1)	M_n (log mol ⁻¹)	176 (Pa s)	7 (0) ^d	nª
Polyethylene	PEI	42	0.982	0	101	39	383	0.021	0.469
Polyethylene	PE2	14	0.962	0	154	42	1,693	2.449	0.186
Polyethylene	PE3	0.9	0.962	0	234	-	14,061	1.143	0.312
Poly(othylene-co-1-octene)	EcO1	5.0	0.868	7.8	172	78	17,401	_	0.167
Puly(athylene-co-I-octana)	EcO2	0.5	0.868	7.7	261	123	42,183	0.001	0.263
Puly(propylane-co-sthylane)	PcE	-	0.860	88	88	-		-	-
Poly(ethylene-co-1-butene)	ReB	0.8	0.880	13	266	120	14,786	0.160	0.584
Poly(ethyleno-alt-propylene)	EaP	-	0.910	60	521	314	6,944	0.078	0.628

[&]quot;Malt-flow index determined in accordance with BS 720A Test Condition 4.

Dennity at 25 °C.

** Olefin content.

Reciprocal transition rate of the Carress aquation (eq. 1).

where η^* is the complex viscosity at angular velocity ω , τ is the reciprocal transition rate (relaxation time), and n is the non-Newtonian exponent (the alope of the viscosity curve in the pseudoplastic region at $\gamma \to \infty$). η^*_{D} , τ , and n were found with the unweighted least sum-of-squares method 17 for the fit of the η^* values experimentally determined through rheometry to the model containing ω as the independent variable:

$$xs_{min} = \sum_{j=1}^{n} \Delta y_{j}^{k} \tag{2}$$

where ss_{min} is the minimum sum of squares of n residuals. Ay, is equal to $\eta^{**} = \eta^{*} = \eta^{*} = is$ the experimental value, and $\eta^{**} = is$ the corresponding value calculated from the model for datum j. The Solver program in Microsoft Excel '97 was used to accomplish this task. For the EcO resin, a better fit of the experimental data was obtained with a modified Carreau equation from Dumoulin et al...

$$\eta_{-}^* = \eta_{0}^* [1 + (\tau \omega)^*]^{-}$$
 (3)

where m is a fitting constant. The blands, listed in Table 2, of PE with the copolymers were prepared with compositions at the critical point, the volume fraction of the copolymer (ϕ_2^c) , from the Flory-Huggins lattice model, as described by Crist and Hill: 10

$$\phi_1^C = [1 + (V_2 n_{w2}/V_1 n_{w2})^{1/2}]^{-1}$$
 (4)

where V_j is the monomer volume and n_{wj} is the weight-average degree of polymerization of component j. On the basis of the free-volume theory, V_j is a function of the expansion coefficient (β) , absolute temperature (T), and glass-transition temperature (T_g) :

$$V_{i} = V_{\text{BREK}} \left[1 + \beta_{\text{EREK}} \left(T - 298 \right) \right]$$
 (5)

where β_{236K} is the thermal expansion coefficient at 298 K [β_{296K} = (298 + 4.23 T_g^{0}). T_g values were determined from thermograms of the heat capacity versus the temperature obtained with a PerkinElmer DSC7 differential scanning calorim-

Table 2. Blond Characteristics at 443 K.

Blend	好	η ₀ * (Pm)	٠,	(MPa ¹⁴)	AC
PK1/Ec01	0.43	910	0.9872	0.02	0.15
PE2/EcO1	0.49	1,656	0.9964	0.02	0.15
PEVE-02	0.39	2,570	0.9963	0.08	0.16
PE2/EcO2	0.44	6,530	0.9879	0.03	0.16
PES/EcO2	0.45	17,026	0.9947	D.03	0.16
PEI/EcB	0.38	2,533	_	0.00	0.05
PE2/EcB	0.43	4.169		0.09	0.05
PENROB	0.45	13,734	_	0.09	0.05
PEVEaP	0.32	793	0.9741	0.43	0.40
PE2/E-P	0.37	2,287	0.9880	0.48	0.40
PE3/EaP	0.39	9.102	0.9798	0.43	0.40
PE1/PeE	0.53	110	0.9710	0.76	0.70
PE2/PcE	0.58	182	0.9696	0.76	0.70

^{*} From Figures 5, 6, and 7.

Courseming not observed.

[&]quot;Slope of the viscosity curve in the pseudoplastic region at y -- * (eq 1)

eter at heating rates of 2, 5, 10, 15, and 30 K min^{-1} . T_s^0 values were obtained by the plotting of T, versus the heating rate and extrapolation to 0 K min⁻¹; the T_s axis intercept was taken as the T_s^0 value, where T_s^0 is the glass transition temperature at a heating rate of 0 K/min. Vaces values were taken from Bicarano. 21 The blands were prepared through the dissolution of the components in toluene at 400 K followed by precipitation through pouring into excess methanol at 303 K. The precipitates were removed from the solvent through filtration and then washed with fresh methanol before drying in vacuo at 333 K for 5 h. The samples were then consolidated, wrapped in aluminum fail, and annealed in an in-house-built tube furnace under a nitrogen gas purge for six time intervals up to 2 h at 443 K. A thermocouple was inserted into the sample to determine the temperature. The samples were then quenched in ice water and were sectioned to a nominal thickness of 1 µm with an RMC microtome operated at -80 °C. The sections were placed on glass alides beneath coverslips, with dioctylphthalate as the mounting madium, and were viewed with a Nikon E400 light microscope employing phase-contrast plates. Images were captured with a Sony CMA-D2CE charge-coupled-device (CCD) camera. The morphology length scale (A) was measured with Imagepro software with standard stereological analysis.23 Test lines were placed over the image, and the length of the test line (x,) traversing each domain was determined. The length scale was then calculated ($\lambda = \sum x/n_{i}$, where n_{i} is the numbor of times the test line crosses a domain).

RESULTS

The $T_{\rm g}^0$ values used to calculate the monomer volumes are documented in Table 3. Because the interaction parameter (χ) was found to be a function of the blend composition, particularly at low and high concentrations of polymer 2, at which a twofold increase could occur, the samples in this work were prepared at the critical composition to limit this effect; ¹⁸ χ was generally nearly constant at compositions close to the critical point.

Upon annealing under quiescent conditions in the melt state at 443 K, the morphologies that formed were cocontinuous, except for the samples containing EcB. For the EcB-containing samples, no coarsening of the morphology was observed; a fine length-scale morphology that did not change over the period of annealing was the result. Fig-

Table 3. Polymer characteristics

Polymer	a (mal %)	(E)	8 (MPa ^{L/8})*	C 7.00*	
PE	0	253.2	14.30		
PP	0	-	13.43	6.20	
P1B*	0	_	13.65	6.60	
P10	0	-	13.97	9.10"	
BaP	50	201.3	13.87	6.80	
BeO1	7.3	201.2	14.28	7.15	
EcO2	7.7	201.2	14.28	7.164	
EcB	18	241.8	14.22	8.964	
PeR	86	248.2	13.54	6.304	

* Glam-transition rate at a zero hanting rate.

Solubility parameter at 443 K calculated from group contrinutions. 47

Characteristic ratio data from Bicorano. **

d Calculated from the values of the homopolymers.

Poly(1-buttone)

Poly(1-octone).

are I shows digitized images of the PE3/EcO2 blend after annealing at 443 K for time intervals of up to 2 h. These images are typical of those obtained of samples that contained the EcOl, EcO2, EaP, and PcE copolymers. The lighter gray regions that appear to stand out in relief are the copolymor-rich regions; the PE-rich material constitutes the darker regions because of its higher crystallinity and, consequently, higher density. A assessed from the CCD images, has been plotted against the annealing time (t) in Figures 2-4 for the blend samples containing PE1, PE2, and PE3 respectively. Apparently, for each grade of PE, the coarsening rates were influenced by the type of copolymer present, the level of coarsening following the sequence PcE > EaP > EcO1 > EcO2> EcB. Moreover, the coarsening progress was affected by the grade of PE present in the bland. To further investigate the coarsening process, we related λ to vector (q) by $\lambda = 2m/q$. The plots of q. on a logarithmic scale, versus the cubed root of t, shown in Figures 5-7 for samples containing PE1, PE2, and PE3, respectively, were found to be masentially linear in the range of 300 < t < 7200 s. Data were fitted to exponential curves of the type q = a exp(bt1/2), where a and b are fitting constants. The correlation coefficients (r) for these fits are listed in Table 2.

Relationships of this type were discussed by Lee and Han. ²³ According to theories of spinodal decomposition. ²⁴ at times close to t=0, q has a constant value of q_m and later shifts with time as coarsening progresses. In separate studies, Inaba

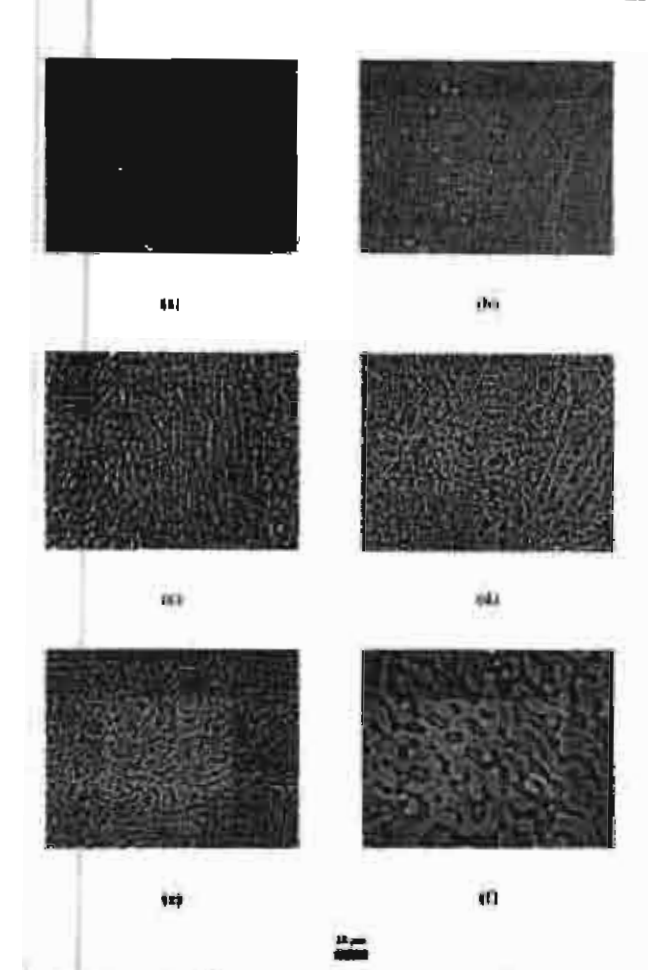


Figure I. CCD camera images, taken with a transmitted light microscope with a phase-contrast plate, of PES/EcO2 after annualing times of (a) 5, (b) 15, (c) 30, (d) 60, (e) 90, and (f) 120 min at 443 K.

et al.²⁵ and Lee and Han²³ reported that the convening in the melt state of immiscible blends after homogenisation through the dissolution of the constituent polymers in a common solvent and rapid precipitation with a nonsolvent was equivalent to phase separation via spinodal decomposition induced by deep quenching of a mait blend from a single-phase condition into two-phase conditions through the control of temperature and, therefore, could be described through established kinetic models. The coarsening rate of the morphology is $R = q^2 D_{app}/2$. The mutual diffusion coefficient (D_{app}) is equal to D_f , D_s being the self-diffusion coefficient of polymer f ($D_s = kM_f^{-2}$, where M_f is the molecular weight and k_f is a constant) and f_s equal to $(\chi - \chi_s/\chi_s)$ being a factor that modifies the diffusion rates due to thermodynamic effects. 25 χ_s is the interaction pa-

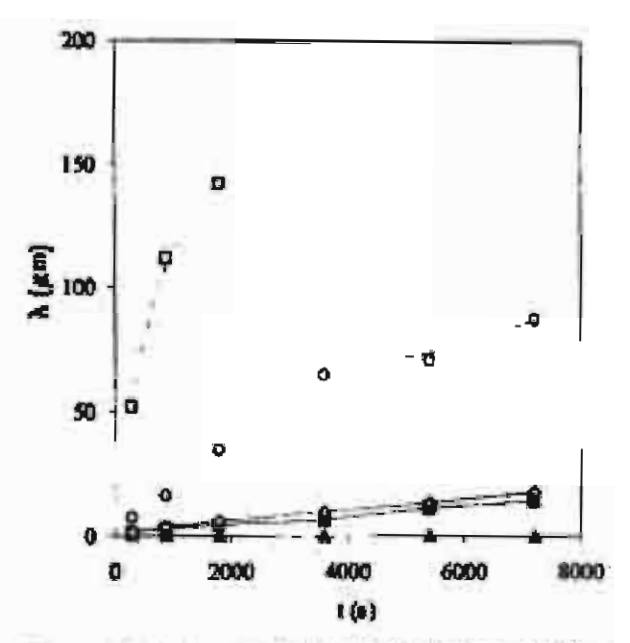


Figure 2. A versus s at 443 K for blends containing PE1 blended with (O) EaP, (A) EcB, (II) PcE, (III) EcO2, and (O) EcO1.

rameter at the spinodal. The zero-shear-rate viscosity and self-diffusion rates are closely related properties, the term (D/Th₀) being insensitive to

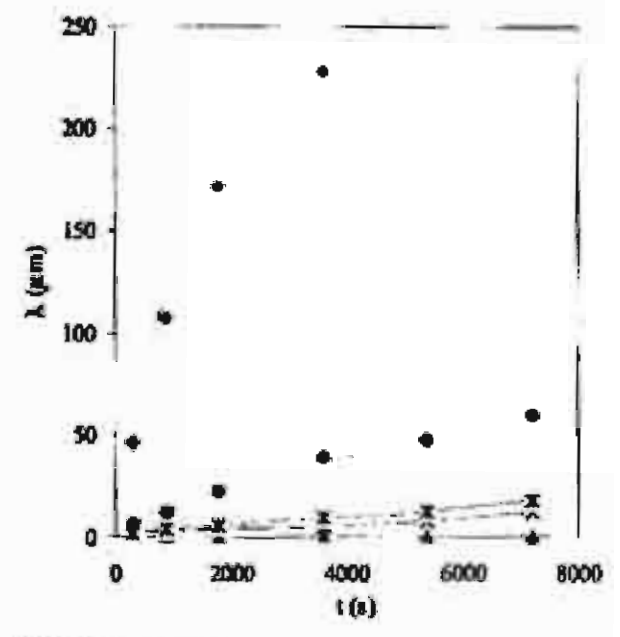


Figure 8. A versus t at 443 K for blends containing PE2 blended with (*) RaP, (A) EcB, (*) PcE, (×) EcO2, and (*) EcO1.

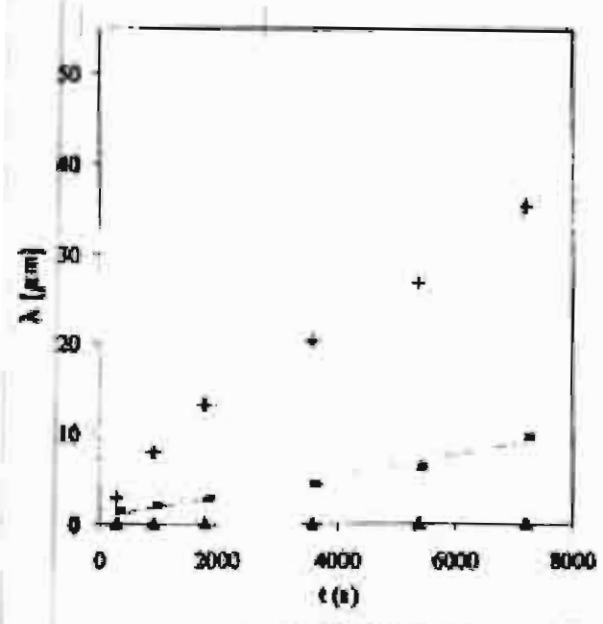


Figure 4. A versus : at 448 K for blends containing PE3 blended with (+) BaP, (4) BeB, and (-) BcO2.

the temperature.²⁶ Thus, $D_* \propto \eta_0^{-1}$, and $R \propto D_{\rm app} \propto \eta_0^{-1} f$. Hydrodynamic effects during the early and late stages of coarsening may be described as follows:

$$\lambda \propto (\lambda_{1} T/\eta_{2})^{1/3} t^{1/3}$$
(6)
$$\lambda \approx (\lambda_{1} T/\eta_{2})^{1/3} t^{1/3}$$
(6)
$$\lambda \approx (\lambda_{1} T/\eta_{2})^{1/3} t^{1/3}$$
(7)
$$\lambda \approx (\lambda_{1} T/\eta_{2})^{1/3} t^{1/3}$$
(8)
$$\lambda \approx (\lambda_{1} T/\eta_{2})^{1/3} t^{1/3}$$
(9)
$$\lambda \approx (\lambda_{1} T/\eta_{2})^{1/3} t^{1/3}$$
(10)
$$\lambda \approx (\lambda_{1} T/\eta_{2})^{1/3} t^{1/3}$$
(11)
$$\lambda \approx (\lambda_{1} T/\eta_{2})^{1/3} t^{1/3}$$
(12)
$$\lambda \approx (\lambda_{1} T/\eta_{2})^{1/3} t^{1/3}$$
(13)
$$\lambda \approx (\lambda_{1} T/\eta_{2})^{1/3} t^{1/3}$$
(14)

Figure 5. q versus $t^{1/3}$ at 443 K for blends containing PE1 blanded with (O) EaP, (II) PcE, (II) EcO2, and (O) EcO1.

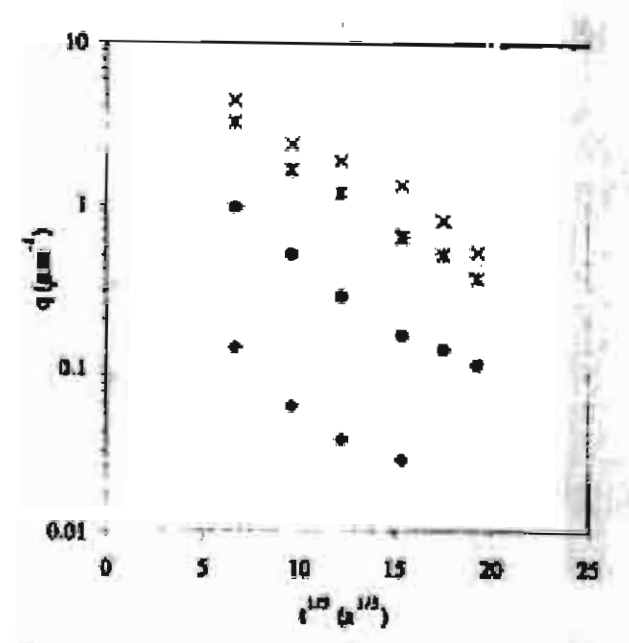


Figure 6. q versus *** at 443 K for blends containing PE2 blunded with (6) HaP, (4) PeE, (×) EcO2, and (*) BcO1.

$$\lambda \propto (\Gamma_1 / \eta_0) \epsilon$$
 (7)

where k_0 is the Boltzmann constant. Thus, the coarsening rates are affected by the melt viscosity

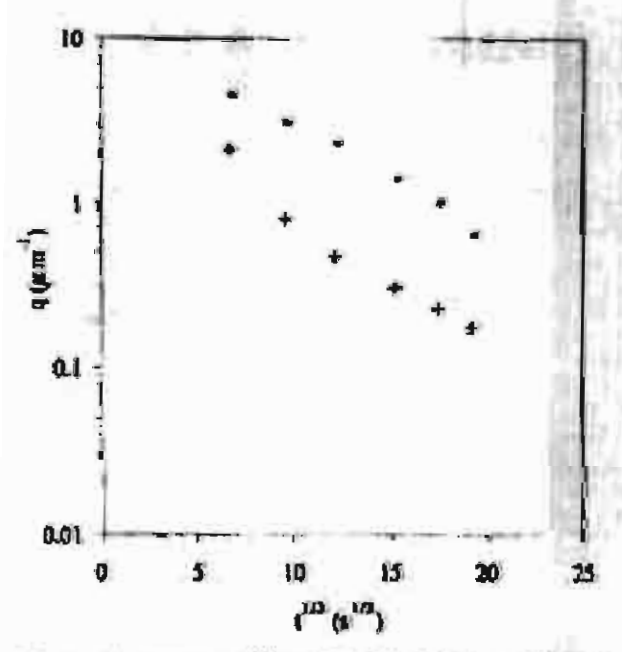


Figure 7. q versus e¹²⁵ at 443 K for blends containing PE3 islanded with (+) BaP and (-) Sc02.

and thermal energy, as well as the mutual compatibility of the blend components. A normalized term (q^*) may be defined as $q^* = q(k_BT/\eta_0^*)^{1/3}$, which encompasses the thermal energy (k_BT) and viscous factors (in the form of η_0^*). The product q^{**} at any time t is a dimensionless number that represents the coarseness of the morphology, being independent of the viscosity and thermal energy.

Typical plots from which the zero-shear-rate visconities were determined are presented in Figure 8. q* is plotted as a function of time in Figure 9. Evidently, after normalization, the data fall on three curves labeled I, II, and III. These curves correspond to the formulations containing PcE. EaP, and EcO, respectively, the gradient and relative position of each curve being determined by the nature of the copolymer. Thus, the normalization of the data in the form of q" largely accounts for the differences in the melt viscosity of the PE and copolymer resins, revealing the influence of the copolymer microstructure. Moreover, the results show that the molecular weights of the PE and copolymer resins have a relatively small offect on the coarsening of the murphology, in comparison with the influence of the copolymer microstructure. The coarsening process represented by the plot of q* versus the reveals the compati-

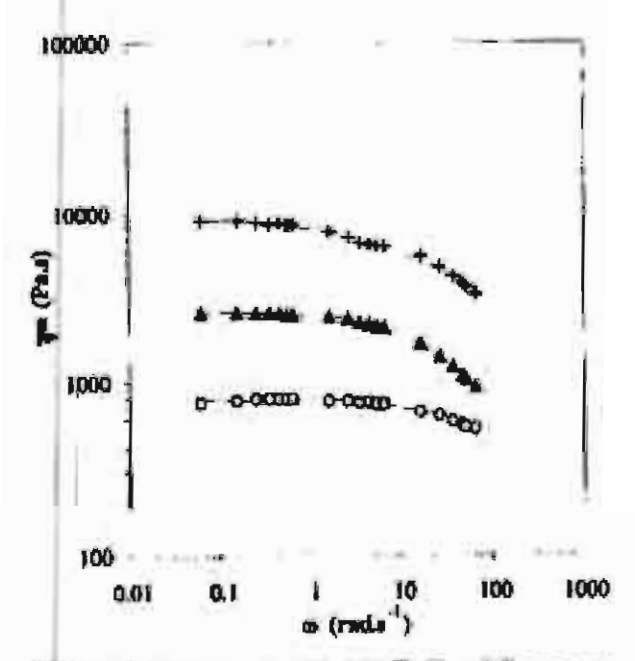


Figure 8. n* versus w at 443 K. Trood lines were calculated with the least sum-of-squares fit of the Carrent equation (eq 1) to the experimental data: (+) PEM EsP. (A) PEMECB, and (O) PEMESP.

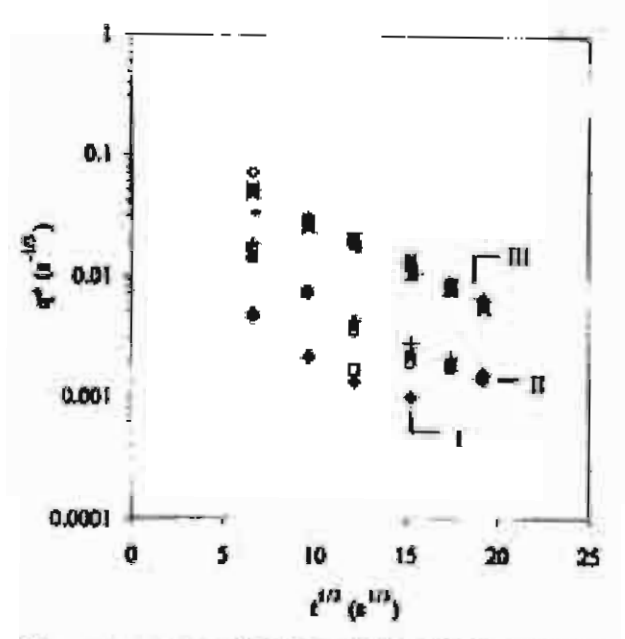


Figure 8. q* as a function of tth at 443 K for blends containing PE1 blended with (O) EaP, (□) PcE, (E) BcO2, and (○) EcO1, samples containing PE2 blended with (O) EaP, (♠) PcE, (×) EcO2, and (°) EcO1, and samples containing PE3 blanded with (+) EaP and (-) EcO2. The curves are grouped into (I) PcE-, (II) EaP, and (III) EcO-containing formulations.

bility between PE and the copolymers, which is independent of the viscosity and thermal energy. A downward shift of q* versus I^{1/3} is a result of decreasing compatibility of the constituent polymer, and so the compatibility of the copolymers with PE follows the sequence EcB > EcO > EaP > PcE.

DISCUSSION

Two principal approaches have been investigated in attempts to describe miscibility in polyplefin blends. In the first approach, mixing has been correlated with the difference in δ of the constituent polymers:⁸ the larger the difference, the lower the compatibility. The focus of the second approach has been to consider differences in the polymer main-chain stiffness. ^{1,5}

 δ may be calculated with group contribution methods.²⁷ In this work, for the homopolymers, δ was calculated from data by Hoy, tabulated by Cowie,²⁷ with the following equation: $\delta = \Sigma F/V$, where F, is the group contribution of functional

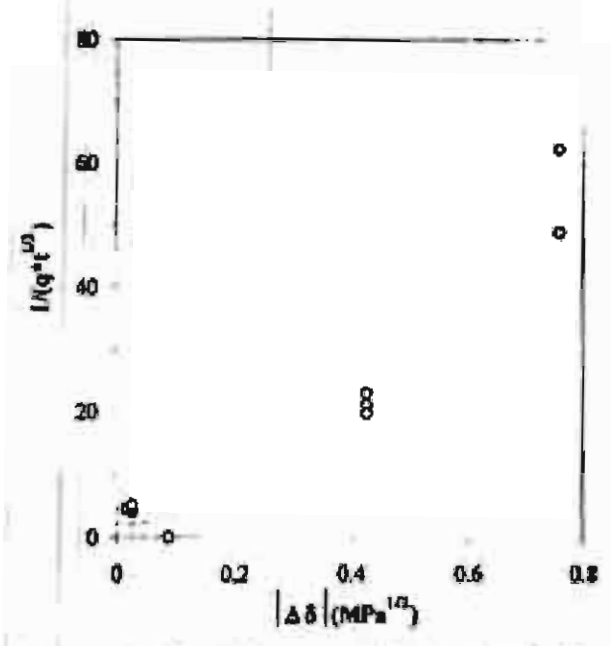


Figure 10. Morphology coursening, represented by $1/(q^4t^{1/3})$, as a function of $|\Delta\delta|$.

group j and V is the molar volume of the polymer repeat unit at 443 K. V was obtained as described in the Experimental section. Data for the copolymera (δ_{Eas}) were calculated: $\delta_{Eas} x_E \delta_{PR} + x_a \delta_{Pa}$, where z is the molar fraction of monomer residue in the copolymer; subscript E denotes ethylane, a represents the a-olefin, and PE and Pa refer to the corresponding values of the PE and poly(aolefin) homopolymers, respectively. The δ values are listed in Table 3. The differences in the 5 values of the components in each blend (A8 = $|\delta_{\rm pg} - \delta_{\rm Eco}|$ are given in Table 2. To correlate $\Delta\delta$ with the coarsening behavior, we arbitrarily selected the q* value at the midpoint of q* versus which corresponded to an annealing time of 30 min. The reciprocal of the product q*t1/3 was then taken because the q*t1/3 value for the EcBcontaining samples was infinity (no coarsening was observed); 1/(q*113) was then zero for EcB samples. L(q*1 1/8) is plotted against | A5| in Figure 10. Broadly, the larger difference in 8 correlates with more extensive coarsening of the marphologies within the annealing time, as indicated by the higher value of L(q*113). However, it fails to reflect the coarser morphologies of the samples containing EcO, in comparison with those containing EcB. Moreover, the increase in the branch length of the copolymer, which results from the increase in the molecular weight of the a olefin commonner residue, brings δ of the copolymer closer to that of PE, and this suggests an increase in the compatibility with PE. The morphology analysis shows the opposite result, with the EcO copolymer coarsening faster than that of the EcB-containing sample, although the former has a lower content of commonner residue and, therefore, fewer branches Small-angle neutron scattering experiments have shown that χ increases as the branch length increases.

Chain stiffness may be described with saveral terms, including the characteristic ratio (C). The values of C, taken from Bicurano, 25 are listed in Table 3. Data for the copolymers were calculated (C_{len}) with $C_{\text{len}} = x_{\text{R}}C_{\text{PR}} + x_{\text{n}}C_{\text{Po}}$. The differances in C between the copolymers and PE (IAC) = |ΔCpg - ΔCgco|) are shown in Table 2; 1/(q*t16) is plotted as a function of |AC| in Figure 11 Apparently, the larger differences in C are associated with the greater levels of coarsening. Much more data are required to determine the generality of this result, however. The correlation between C and & are controlled by the same factors related to the polymer structure, and so the results may be confounding the underlying phepomens that control the mixing and coarsening of the polymer blends. As pointed out by Crist and Hill, 19 these simple structural factors, 8 and C. ere inadequate for describing the compatibility of polyclefins when the polymers are very similar in

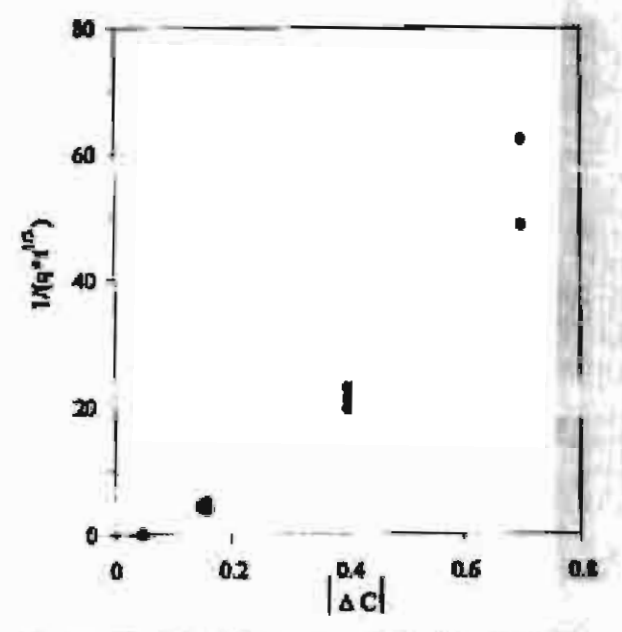


Figure 11. Morphology coarsening, represented by $1/(q^{-1/2})$, as a function of $|\Delta C|$.

structure and approach the limits of miscibility. As evidenced in this report, EcO and EcB have close values of 5 and C and yet exhibit markedly different compatibilities with linear PE.

CONCLUSIONS

The coarsening rates of linear PE with five poly-(othylene-co-o-olefin) elastomers with compositions at the critical point were normalized to account for the effects of the thermal energy and zero-shear-rate viscosity. The influence of the molecular weight on the morphology evolution was principally through its effect on the melt viscosity, with little effect on the thermodynamic compatibility. The coarsening progress of the morphology was related to the copolymer microstructure and branch content. The faster coarsening rates were associated both with the largest differences in 8 and with the largest differences in C between PE and the poly(ethylene-co-o-olefin) copolymers. However, the marked differences in coarsening between EcB and EcO were not well reflected by the small differences in δ and C.

Financial support from the Thailand Research Fund through the Golden Jubilee Ph.D. Program (PHD/0012/ 2544) to N. Phachalam and R. Venables is acknowledged.

REFERENCES AND NOTES

- Bates, F. S.; Schulz, M. F.; Rosedale, J. H. Macromolecules 1992, 25, 5547-5550.
- Rhee, J.; Crist, B. Marzomolecules 1991, 24, 5663-5669.
- Choi, P. Polymer 2000, 41, 8741-8747.
- Krishnamoorti, R.; Graessley, W. W.; Balsara, N. P.; Lohse, D. J. Macromolecules 1994, 27, 3073– 3081.
- Fredrickson, G. H.; Liu, A. J. J Polym Sci Part B: Polym Phys 1995, 33, 1208–1212.
- Yamaguchi, M.; Miyata, H.; Nitta, K. J Appl Polym Sci 1996, 62, 87.

- Thomson, Y.; Suhm, J.; Thomson, R.; Bar, G.; Maier, R. D.; Mulhaupt, R. Macromolocules 1988, 31, 5441.
- Carriere, C. J.; Silvia, H. C. J Appl Polym Sci 1997, 66, 1176.
- Morgan, R. L.; Hill, M. J.; Barham, P. J.; Frye, C. J. Polymer 1997, 38, 1903.
- 10. Hill, M. J.; Barham, P. J. Polymer 1995, 36, 3369.
- Rhee, J.; Crist, B. J Polym Sci Part B: Polym Phys. 1994, 32, 159-169.
- Saunders, K. J. Organic Chemistry of Polymers,
 2nd ed.; Chapman & Hall; London, 1988; pp 46-75.
- Chien, J. C. W.; He, D. J Polym Sci Part A: Polym Chem 1901, 29, 1585–1893.
- Halaza, A. F.; Massie, J. M.; Ceresa, R. J. In Science and Technology of Rubber, 2nd ed.; Mark, J. E.; Erman, B.; Eirich, F. R., Eds.; Academic Sun Diego, 1994; p 518.
- De Pooter, M.; Smith, P. B.; Dohrer, K. K.; Bennett, K. F.; Mondows, M. D.; Smith, C. G.; Schouwenaars, H. P.; Geerards, R. A. J Appl Polym Sci 1991, 42, 399–408.
- Carreau, P. J. Ph.D. Thesis, University of Wisconsin, 1968.
- 17. Harris, D. C. J Chem Educ 1998, 75, 119.
- Dumoulin, M. M., Utracki, L. A., Carresu, P. J. Two-Phase Polymer Systems; Hanser Munich, 1991; p 201.
- Crist, B.; Hill, M. J. J Polym Sci Part B: Polym Phys 1997, 35, 2329—2353.
- Cowie, J. M. G. Polymers: Chemistry and Physics of Modern Materials, 2nd ed.; Blackie: London, 1991; p 265.
- Bicerano, J. Prodiction of Polymer Properties; Marcel Dekker: New York, 1993; pp 66-70.
- Dehoff, R. T. Quantitative Microscopy, McGraw-Hill: New York, 1968; p 131.
- 23. Les. J. K.; Han, C. D. Polymer 1999, 40, 2521-2535.
- 24. Cahn, J. W. J Chem Phys 1965, 42, 93.
- Inabe, N.; Yamada, T.; Suzuki, S.; Hashimoto, T. Macromolecules 1988, 21, 407–414.
- Bartela, C. R.; Crist, R.; Gresseley, M. W. Macro-molecules 1984, 17, 2702.
- Cowie, J. M. G. Polymers: Chemistry and Physics of Modern Materials, 2nd ed.; Blackie: London, 1991, pp 178–179.
- Bicerano, J. Prediction of Polymer Properties, Marcel Dekker, New York, 1993; p 286.

structure and approach the limits of miscibility. As evidenced in this report, EcO and EcB have close values of 8 and C and yet exhibit markedly different compatibilities with linear PE.

CONCLUSIONS

The coarsening rates of linear PE with five poly-(ethylene-co-a-olefin) elastomers with compositions at the critical point were normalized to account for the effects of the thermal energy and zero-shear-rate viscosity. The influence of the molecular weight on the morphology evolution was principally through its effect on the melt viscosity, with little effect on the thermodynamic compatibility. The coarsening progress of the morphology was related to the copolymer microstructure and branch content. The faster coarsening rates were associated both with the largest differences in 8 and with the largest differences in C between PB and the poly(ethylene-co-a-olefin) copolymers. However, the marked differences in coarsening between EcB and EcO were not well reflected by the small differences in δ and C.

Financial support from the Thailand Research Fund through the Golden Jubiles Ph.D. Program (PHD/0012/ 2544) to N. Phochalam and R. Vonables is acknowledged.

REFERENCES AND NOTES

- Bates, F. S.; Schulz, M. F.; Resedule, J. H. Macromolecules 1992, 25, 5547-5650.
- Rhee, J.; Crist, B. Macromolecules 1991, 24, 5663– 5669.
- 3 Choi, P. Polymer 2000, 41, 8741-8747.
- Kriehnamoorti, R.; Graceley, W. W.; Balaara, N. P.; Lohse, D. J. Macromolecules 1994, 27, 3073— 3081.
- Fredrickson, G. H.; Liu, A. J. J Polym Sci Part B: Polym Phys 1995, 33, 1203-1212.
- Yamaguchi, M.; Miyata, H.; Nitta, K. J Appl Polym Sci 1996, 62, 87.

- Thomann, Y.; Suhm, J.; Thomann, R.; Bar, G.; Maier, R. D.; Mulhaupt, R. Macromolecules 1996, 31, 5441.
- Carriere, C. J.; Silvia, H. C. J Appl Polym Sci 1997, 66, 1175.
- Morgun, R. L.; Hill, M. J.; Barham, P. J.; Frye, C. J. Polymer 1997, 38, 1908.
- 10. Hill, M. J.; Barham, P. J. Polymer 1995, 36, 3369.
- Rhee, J.; Crist, B. J Polym Sci Part B: Polym Phys. 1994, 32, 159-169.
- Saunders, K. J. Organic Chemistry of Polymers,
 2nd ed.; Chapman & Hall: London, 1988; pp 48-75.
- Chien, J. C. W.; He, D. J Polym Sci Part A: Polym Chem 1991, 29, 1585–1593.
- Halasa, A. F.; Massie, J. M.; Ceresa, R. J. In Science and Technology of Rubber, 2nd ed.; Mark, J. E.; Erman, B.; Eirich, F. B., Edu.; Academic: San Diego, 1994; p 518.
- De Pooter, M.; Smith, P. B.; Dohrer, K. K.; Bennett, K. F.; Meadows, M. D.; Smith, C. G.; Schouwennars, H. P.; Geerards, R. A. J Appl Polym Sci 1991, 42, 399-408.
- Currenu, P. J. Ph.D. Thesis, University of Wisconsin, 1968.
- 17. Harrie, D. C. J Chem Educ 1998, 75, 119.
- Dumoulin, M. M.; Utracki, L. A.; Carreso, P. J. Two-Phase Polymer Systems; Hanser: Munich, 1991; p 201.
- Crist, B.; Hill, M. J. J Polym Sci Part B: Polym Phys 1997, 35, 2329-2353.
- Cowie, J. M. G. Polymers: Chemistry and Physics of Modern Materials, 2nd ed.; Blackie: Landon, 1991; p 265.
- Bicerano, J. Prediction of Polymer Properties, Marcel Dekker: New York, 1993; pp 66-70.
- Dehoff, R. T. Quantitative Microscopy; McGraw-Hill: New York, 1968; p 131.
- 23. Lee, J. K.; Han, C. D. Polymer 1999, 40, 2521-2536.
- 24. Cahn, J. W. J Chem Phys 1965, 42, 93.
- Inaba, N.; Yamada, T.; Suxuki, S.; Hashimoto, T. Macromolecules 1988, 21, 407-414.
- Bartels, C. R.; Crist, B.; Grasseley, M. W. Macromolecules 1984, 17, 2702.
- Cowie, J. M. G. Polymers: Chemistry and Physics of Modern Materials, 2nd ed.; Blackie: London, 1991; pp 178–179.
- Bicerano, J. Prediction of Polymer Properties; Marcel Dekker: New York, 1993; p 286.

